REPORT DOCUMENTATION PAGE

Form Approved
OMB No. 0704-0188

1. REPORT DATE *(DD-MM-YYYY)*	2. REPORT TYPE	3. DATES COVERED *(From - To)*
07/21/2009	Final Performance Report	01/01/2006 to 05/31/2009

4. TITLE AND SUBTITLE

Proteomic Analyses of Cellular Events Mediating/Inhibiting Chemical-Induced Injury

5a. CONTRACT NUMBER

5b. GRANT NUMBER
FA9550-06-1-0083

5c. PROGRAM ELEMENT NUMBER

6. AUTHOR(S)

Frank A. Witzmann, Ph.D.

5d. PROJECT NUMBER

5e. TASK NUMBER

5f. WORK UNIT NUMBER

7. PERFORMING ORGANIZATION NAME(S) AND ADDRESS(ES)

Department of Cellular & Integrative Physiology
Indiana University School of Medicine
Biotechnology Research & Training Center
1345 W. 16th St., Room 308
Indianapolis IN 46202

8. PERFORMING ORGANIZATION REPORT NUMBER

9. SPONSORING / MONITORING AGENCY NAME(S) AND ADDRESS(ES)

AFOSR/NL
801 North Randolph Street Room 732
Arlington VA 22203-1977

10. SPONSOR/MONITOR'S ACRONYM(S)
AFOSR/PK2

11. SPONSOR/MONITOR'S REPORT NUMBER(S)

12. DISTRIBUTION / AVAILABILITY STATEMENT

Approval for public release; distribution is unlimited.

13. SUPPLEMENTARY NOTES

14. ABSTRACT

This project used a proteomic approach consisting of two-dimensional electrophoresis and mass spectrometry to analyze differential protein expression in response to formalin,JP-8 jet fuel, and carbon nanoparticle exposure. The aims were to assess the effect of various chemical exposures both in vivo and in vitro as a means to determine the utility of proteomic approaches in chemical toxicologic investigation. The results suggest that a comprehensive proteomic approach that includes both electrophoretic and mass spectrometric analyses can provide mechanistic information regarding chemical effects, and that the approach can generate additional hypotheses regarding individual chemical effects for further investigation. This is particularly true when proteomic data is combined with toxicological endpoint data and functional analyses.

15. SUBJECT TERMS

16. SECURITY CLASSIFICATION OF:			17. LIMITATION OF ABSTRACT	18. NUMBER OF PAGES	19a. NAME OF RESPONSIBLE PERSON
a. REPORT	b. ABSTRACT	c. THIS PAGE			Frank A. Witzmann
UNCLASSIFIED	UNCLASSIFIED	UNCLASSIFIED			19b. TELEPHONE NUMBER *(include area code)* 317-278-5741

Standard Form 298 (Rev. 8-98)
Prescribed by ANSI Std. Z39.18

1 Introduction

The overall goal of this project was to analyze protein expression profiles of cells exposed to formalin, JP-8 jet fuel, and carbon nanoparticles using proteomics to better understand the nature of their toxicity at the molecular (protein) level, and in the case of formalin, to determine the effect of treatment with a substance P analog (SPa) (Sar^9, Met $(O_2)^{11}$-substance P) in ameliorating the injurious effects. Specifically, two-dimensional electrophoresis (2DE) and mass spectrometry were used to separate, detect, quantify, and identify proteins in whole lung, or lung and kidney cells whose expression was altered in some way by exposure. Samples from exposed (*in vivo* and *in vitro*) lungs and pulmonary epithelial cells (in cooperation with the Witten Lab, U. of Ariz.) and murine kidney cells (in cooperation with the Blazer-Yost Lab, IUPUI) were obtained and cell lysate proteins studied. With an emerging interest in potential intervention by SPa in the pulmonary effects of JP-8 exposure, studies incorporating SPa treatment along with JP-8 exposure were also conducted. An additional, emerging goal became the improvement of sensitivity and dynamic range of the analyses, as the limits of the 2DE technique became apparent. Several improvements in the approach to sample preparation were made. The results of these experiments are summarized in this report. All figures and tables referred to in the text appear at the end of this document in the Appendix.

2 Methods

2.1 Cell Culture/Animal Exposures

2.1.1 Formalin and Sar^9, Met $(O_2)^{11}$-substance P analog (SPA) Study

Fischer 344 male rats (approximately 6 weeks of age and average weight of 172 g) were randomly assigned to either a control (n=6) group, formalin exposure-only group (n=6), or a formalin exposure + SPa treatment group (n=6). The rats were anesthetized for the aerosol administration of formalin or the vehicle control (sterile, normal saline). The SPa + Formalin rats were administered an average of 35 ppm aerosolized 10 µM Sar^9, Met $(O_2)^{11}$-substance P analog over a 10 minute period immediately before formalin exposure as measured by a seven-stage cascade impactor attached to the IN-TOX animal exposure chamber. A mean aerosolized formalin concentration of 67 mg/m^3 (equal to 67 ppm) was used to induce lung injury in the rats over a 1.5 minute volatilization period using an IN-TOX jet nebulizer system. At a mean time of 42 minutes post-formalin exposure, rat lungs were removed and frozen for 2-DE.

2.1.2 Lung Function Test

Lung function in replicate rats was characterized as described previously [1]. The rats were anesthetized with an intramuscular injection mixture of ketamine hydrochloride (80 mg/kg), xylazine (10 mg/kg), and acepromazine maleate (3 mg/kg). A tracheostomy was performed, with the insertion of a Teflon intravenous catheter (20 gauge; Critikon, Tampa Bay, FL) serving as an endotracheal tube. The mice were placed under pressure-controlled respiration (Kent Scientific, Litchfield, CT) and were given an intraperitoneal injection of gallamine triethiodide (8 mg/kg) to suppress spontaneous breathing. Airflow was measured with a pneumotachograph (Fleisch no.

0000, Instrumentation Associates) that was coupled to a differential pressure transducer (Validyne, Northridge, CA). Airflow and pressure signals were used to measure dynamic compliance, and pulmonary resistance was measured with a modified PEDS-LAB (Medical Associated Services, Hatfield, PA) pulmonary function system by the method of Rodarte [2]. Pulmonary function measurements were normalized to individual animal weight. After pulmonary function recording, respiratory permeability was determined by measuring the pulmonary clearance of intratracheally instilled ^{99m}Tc-DTPA. The rats were then sacrificed by exsanguination of the abdominal aorta and the lungs were either flash-frozen for future chemical mediator analyses and proteomics or processed for electron microscopy.

2.1.3 Alveolar Type II (AEII) Cells. A transformed rat AIIE cell line, RLE-6TN was maintained in BRFF-RLuE culture media (BRFF, Ijamsville, MD) containing 10% fetal bovine serum and penicillin/streptomycin antibiotics (pen./strep., Sigma, St. Louis, MO). Cells were cultured in 12-well plates (Fischer Scientific, Pittsburgh, PA) at a density of 10^5 cells/ml. Cell media was replenished every 24–30 h until 95% confluence was achieved and the JP-8 exposures commenced. In all the conditions used in the tests, cell viability, as determined by trypan blue exclusion, was >95% [3].

JP-8 jet fuel was dissolved in BRFF-RLuE media in 1 µl of 100% ethanol as vehicle and dissolved in media to obtain the appropriate concentrations. Control AIIE cultures had cell culture media alone or cell culture media with EtOH vehicle. BRFF-RLuE media was removed from cell culture wells and replaced with either control media or JP-8 jet fuel-supplemented media. Cells were then incubated in media for 24 h at which time the media was removed and samples were frozen at −70 °C until cytokine analyzes. Frozen plates (-80°C) with cells adhering were shipped over night on dry ice to Indiana Univ. for 2-DE analysis.

2.1.4 Carbon Nanoparticle Study

mpkCCD$_{cl4}$ cells were grown in a humidified chamber at 37°C and 5% CO_2. The cell line was maintained in plastic culture flasks and, for experiments, cells were seeded onto Transwell filters or 6-well tissue culture plates. The media was replaced thrice weekly and consisted of Dulbecco's modifed Eagle's medium (DMEM): Ham's F12 base media supplemented with 2% fetal bovine serum, 1 mM Glutamax, 25 U/mL penicillin, 25 mg/mL streptomycin, 12 mg/L ciprofloxacin, 5 mg/L transferrin, 20 µg/L sodium selenide, and 10^{-7} M triiodothyronine.

SWCNT, MWCNT, and C_{60} were first sterilized by mixing in ethanol. After evaporation of ethanol under an ultraviolet germicidal lamp, the CNP were then diluted in fetal bovine serum to 5 mg/mL. Initially, CNP were diluted for each experiment in tissue culture media by vortexing. Later, to increase the efficiency of the CNP suspension, CNP/media mixing used sonication for electrophysiological, imaging, and LFQMS studies. Specifically, CNP were sonicated in FBS, sterilized via autoclave and diluted to 2% FBS-CNP in media and then diluted for each experiment. Cells were exposed to non-sonicated CNP at doses of 200 µg/cm^2 for 24 h in initial 2-DE studies and, in later experiments, exposed to sonicated CNP for 48 h at 20 µg/cm^2 or at 4 µg/cm^2 three times over 7 d.

2.2 Sample preparation for proteomic analysis

2.2.1 Type II alveolar epithelia and mpkCCD$_{cl4}$ cells

All cultured cells were solubilized directly in-well (in situ) after removal of medium. 400 µL of lysis buffer containing 9 M urea, 4% Igepal CA-630 (octylphenoxy polyethoxyethanol), 1% DTT and 2% carrier ampholytes (pH 8–10.5) were added directly to each well. The culture plates were then placed in a 37°C incubator for 1 h with intermittent manual agitation. After 1 h, the entire volume was removed from each well and placed in 2 mL Eppendorf tubes. Each sample was then sonicated with a Fisher Sonic Dismembranator using 3 x 2 s bursts. Sonication was carried out every 15 min for one hour after which the fully solubilized samples were transferred to a cryotube for storage at –80°C until thawed for analysis.

2.2.2 Lung tissue preparation

Frozen lung samples were weighed, and 250 mg pieces placed in 50 mL beakers, along with 8 volumes of a solution containing 9 M urea, 4% Igepal CA-630 ([octylphenoxy] polyethoxyethanol), 1% DTT and 0.2% carrier ampholytes (pH 3-10), and thoroughly minced with surgical scissors. The minced samples were then placed in 3 mL DUALL® (Kimble/Kontes, Vineland, NJ) ground-glass tissue grinders and manually homogenized. After complete solubilization at room temperature for 120 min, samples were centrifuged at 100,000 x g for 30 min using a Beckman (Fullerton, CA,) TL-100 ultracentrifuge to remove nucleic acid and insoluble materials, and the supernatants stored at -45°C until 2-DE separation. Protein concentration was determined using amido black 10B [4], an approach that enables the sensitive and accurate assay of solubilized proteins to be performed without interference from constituents of the lysis buffer.

2.3 Two-dimensional electrophoresis

2.3.1 First-dimension isoelectric focusing

24 cm IPG strips of broad (3-10) pH ranges were rehydrated with 500 µL of sample and focused using the Protean II IEF cell (Bio-Rad). For optimal separation, the strips were passively rehydrated with the solubilized sample for 24 hours. Subsequently, they were focused for 120,000 volt-hours using the following progression: 150 V - 2 hrs; 300 V - 3 hrs; 1500 V - 2 hrs; 5000 V - 7 hrs, 7000 V - 7 hrs, 8000 V - 5 hours at a constant temperature of 20°C. Each strip was equilibrated in 6M Urea, 0.375 M Tris pH 8.8, 4% SDS, 20% glycerol, 2% (w/v) DTT followed by an equilibration in 6M Urea, 0.375 M Tris pH 8.8, 4% SDS, 20% glycerol, 2.5% (w/v) iodoacetamide, then placed on a second-dimension DALT slab gel with a gradient of 11-19% acrylamide.

2.3.2 Second-dimension SDS Slab gel electrophoresis

The second-dimension run was conducted at 160 V for 19 hrs in an ISO-DALT electrophoresis chamber. Twenty second dimension gels were run simultaneously in each gel tank to greatly reduce gel-gel variation. Gels were stained using colloidal Coomassie blue (lower detectable limit, 10-20 ng/spot).

2.3.3 Image Analysis

After staining the gels, protein patterns were analyzed and individual proteins identified using either the GS-800 scanner (BioRad) and PDQuest™ image acquisition and analysis software. Gel patterns were analyzed for both protein quantitation and charge modification by generating a reference 2D pattern that serves as a template to which each 2D protein pattern in the match set (conceivably 20-100 gel patterns, e.g. the "object" patterns) was matched. The reference pattern was constructed by using a representative pattern in one of the groups of gels and assigning a number (SSP) to each detected spot. Correspondence of a protein spot in an object pattern to its counterpart in the master was accomplished by associating the spot number (SSP) in the reference pattern to the object spot. The abundance measurements from each pattern were normalized to correct for slight variations in sample loading or overall stain performance using standard procedures within PDQuest.

2.3.4 Statistical Analysis. Raw quantitative data for each protein spot was exported to Excel for statistical analysis and group comparisons using an unpaired, two-tailed Student's t-test.

2.4 Protein identification and characterization

2.4.1 Peptide Mass Fingerprinting. Protein spots from replicate gels were excised manually, and processed automatically using the multifunctional MultiProbe II Station robot (PerkinElmer). In this automated system, the excised protein spots were de-stained, reduced with dithiothreitol, alkylated with iodoacetamide, and tryptically digested using Promega sequence grade, modified trypsin in preparation for matrix-assisted laser desorption ionization mass spectrometry (MALDI-MS) of the resulting peptides. The peptides were then eluted, cleaned-up/desalted and pre-concentrated by micro solid phase extraction using disposable ZipTip® technology and manually spotted on the MALDI-MS sample target along with α-cyano-4-hydroxycinnamic acid matrix. The MALDI target was then analyzed directly by MALDI-MS using the M@LDI™ (Waters) system. This reflectron/time-of-flight instrument enables the automated acquisition of optimized peptide mass spectra, monoisotopic peptide mass fingerprint determination, and subsequent online interrogation of the ProFound™ Peptide Mass Database. Profound™ calculates the probability that a candidate in a database search is the protein being analyzed. The Z score is calculated when the result of the input mass search is compared against an estimated random match population, and thus corresponds to the percentile of the search in the random match population. For example, a Z score of 1.65 for a search means that the identified protein is in the 95th percentile and only 5% of random matches would yield a higher Z score than this particular set of masses. This is a more readily understandable way of expressing the robustness of a protein identification obtained by peptide mass fingerprinting.

2.4.2 Mass spectrometric identification of 2-D gel protein spots.

2.4.2.1 In-gel Tryptic Digestion

Each pre-selected detectable protein spot that could be detected was cut manually

from each of four separate gels by hand using a 1.5 mm gel cutting tool on a light box. The four replicate gel plugs were placed in one well of a 96-well plate and processed using the MultiProbe II (Perkin-Elmer, Boston MA). In this automated system, the excised protein spots were first destained first with 50 mM ammonium bicarbonate-50% acetonitrile followed by 100% acetonitrile. Protein reduction with 10 mM DTT and alkylation with 55 mM iodoacetamide were carried out, followed by overnight tryptic digestion using modified trypsin at 6 ng/µl at and 37oC with shaking, using modified trypsin at 6 ng/µl. The resulting peptides were extracted from gel plugs with vigorous shaking via Jitterbug (Boekel Scientific) for 20 min in two rounds of the following three phases: 1) 15 µl 0.2% formic acid and 15 µl of acetonitrile solution (50% aqueous), 2) 21 µl 0.2% formic acid and 9 µl of acetonitrile solution (70% aqueous), and 3) with 30 µl of acetonitrile solution (0% aqueous). After each phase, the extraction solution was placed in a separate 96 well plate and dried via speedvac without heat. The dehydrated peptides were then reconstituted in 20 µL of 0.1% trifluoroacetic acid with continuous shaking for 5 minutes before being concentrated and desalted using µ-C-18 Millipore ZipTip® pipette tips (Billerica, MA) according to the manufacturer's protocol. Purified peptides were eluted in a new 96 well plate, dried via speedvac, and then reconstituted in 5% acetonitrile and 0.1% formic acid.

2.4.2.2 LC-nESI-MS/MS

Peptide samples (40 µL) were injected (40 µL) into a Thermo Scientific LTQ linear ion trap mass spectrometer using a Michrom Paradigm AS1 auto-sampler coupled to a Paradigm MS4 HPLC (Michrom BioResources, Inc., Auburn, CA). The peptide solution was automatically loaded at a flow rate of 0.5 µL/min across a Paradigm Platinum Peptide Nanotrap (Michrom BioResources, Inc., Auburn, CA) and onto a 150 mm X 0.099 mm capillary column (Polymicro Technologies, L.L.C., Phoenix, AZ) packed in house using a 5 µm, 100 Å pore size Magic C18 AQ stationary phase (Michrom BioResources, Inc., Auburn, CA). The mobile phase A, B, and C were 2% acetonitrile in 0.1% formic acid, 98% acetonitrile in 0.1% formic acid, and 5% acetonitrile in 0.1% formic acid, respectively, all in HPLC grade water. Buffer C was used to load the sample, and the gradient elution profile was as follows: 5% B (95% A) for 10 min; 5-55% B (95-45% A) for 30 min; 55-80% B (45-20%A) for 5 min; and 80-5% B (20-95% A) for 10 min. The data were collected in a "Triple-Play" (MS scan, Zoom scan, and MS/MS scan) mode using a nanospray interface (NSI) with a normalized collision energy of 35%.

2.4.2.3 Bioinformatic Analysis of Identified Proteins

The acquired mass spectral data were searched against a FASTA format database created assembled in- house using gene annotations publicly available from PIR (Protein Information Resource, http://pir.georgetown.edu/) using the SEQUEST (v. 28 rev. 12) program in Bioworks (v. 3.3). General parameters were set as follows: peptide tolerance 2.0 AMU, fragment ion tolerance 1.0 AMU, enzyme limits set as "fully enzymatic – cleaves at both ends" and missed cleavage sites set at 2. The searched peptides and proteins were subjected to the validation processes PeptideProphet [22] and ProteinProphet [23] in the Trans-Proteomic Pipeline (TPP, v. 3.3.0) (http://tools.proteomecenter.org/software.php), and only those proteins with greater than

90% confidence (containing multiple peptides with greater than 90% confidence) were considered positive identifications.

2.4.3 Electrophysiological and Imaging Studies

Electrophysiological techniques were used to monitor TEER. Cells were grown to confluency over a period of 14 days on Transwell filters with CNP treatment as indicated in the figures. The filters were excised, mounted in a Ussing chamber, as described in detail previously [8]. The spontaneous transepithelial potential difference across the monolayer was measured and clamped to zero. The resulting short circuit current is a measure of net ion flux. Every 200 seconds, the zero holding potential was changed to a different holding potential and the resulting deflection in the short-circuit current (SCC) was measured and used to calculate the TEER by Ohm's law.

For imaging, replicate cellular monolayers were washed, blocked, exposed to mouse monoclonal PCNA antibodies overnight at 4°C, washed, and exposed to goat anti-mouse Alexofluor 488 secondary antibody. Another set of cells were exposed to Rhodamine-phalloidin and DAPI. All cells were visualized using a Nikon Eclipse TE2000-U Microscope fitted with a Nikon Digital Camera.

2.4.4 Label-free Quantitative Mass Spectrometry

Replicate cell samples were tryptically-digested and the peptides injected onto an Agilent 1100 nano-HPLC system (Agilent Technologies, Inc., Santa Clara, CA) with a C18 capillary column in random order. Peptides were eluted with a linear gradient developed over 120 min and the effluent electro-sprayed into the LTQ mass spectrometer. Data were collected in the "Triple-Play" (MS scan, Zoom scan, and MS/MS scan) mode. Database searches against the International Protein Index (IPI) human database and the Non-Redundant-homo sapiens database were carried out using both the X!Tandem and SEQUEST algorithms. Protein quantification was carried out using an established algorithm [5-7] to which we have access. Briefly, when the raw files were acquired from the LTQ mass spectrometer, all extracted ion chromatograms (XICs) were aligned by retention time. To be used in the protein quantification procedure, each aligned peak must have a matched precursor ion, charge state, fragment ions (MS/MS data) and retention time (within a one-minute window). After alignment, the area-under-the-curve (AUC) for each individually aligned peak from each sample was measured, normalized, and compared for relative abundance. After obtaining the list of proteins that are differentially expressed after CNT exposure, a corresponding gene list was created for bioinformatics analysis.

Because the data has multiple sources of random variation (biological and technical), a Linear Mixed Model (a generalization of an ANOVA) was used for biostatistical analysis in this study. In general, significant technical variation is introduced by the act of 'measurement' in most 'omics' studies. Randomization of measurement order and normalization of the data eliminates the technical bias. We used a statistically-based quantile normalization method for data normalization on a log scale. Log base 2 was chosen because a unit difference on the log scale is equivalent to a two-fold change. A byproduct of the Linear Mixed Model is a p-Value or measure of significance for an observed change in protein expression (signal). The p-Value estimates the proportion of times a change that large will be observed if in fact there is

no real change (the False Positive Rate). All p-Values were transformed into q-Values that estimate the False Discovery Rate (FDR). For each protein a separate analysis of variance (ANOVA) model was fit:

$$\text{Log 2 (Intensity)} = \underset{\text{(Fixed)}}{\text{Group Effect}} + \underset{\text{(Random)}}{\text{Sample Effect}} + \underset{\text{(Random)}}{\text{Replicate Effect}}$$

Log2 (Intensity) is the protein intensity based on the weighted average of the quantile normalized log2 peptide intensities with the same protein identification. *Group Effect* refers to the fixed effects (not random) caused by the experimental conditions or treatments that are being compared. *Sample Effect* (nested within a group) refers to the random effects from individual biological samples. It also includes the random effects from the individual sample preparations. *Replicate Effect* (nested within sample) refers to the random effects from replicate injections from the same sample preparation (each sample was injected twice).

3 Results & Discussion

3.1. Formalin, SPa, and Lung Injury

3.1.1 Pulmonary Function

As explained in the methods section replicate rats were subjected to pulmonary function tests. The formalin-exposed rats demonstrated a 33-fold increase in inspiratory dynamic lung compliance (mL/cm H_2O) compared to the formalin + SPa rats (Table 1). This large increase in inspiratory dynamic lung compliance was accompanied by a 6.32-fold increase in lung permeability as measured by 99mTc-DTPA (diethylenetriamine-pentaacetic acid) clearance in the formalin rats compared to the formalin + SPa group (Table 2).

3.1.2 Lung Pathology

A pathological examination of the excised lungs revealed injury to the alveolar-capillary membranes and cell destruction in the formalin rats compared to the SPa-treated rats (Figure 1). The damaged alveolar-capillary membranes are consistent with the increased lung permeability indicated by the 6.32-fold increase in 99mTc-DTPA clearance in the formalin rats versus the formalin + SPa-treated group. Most of the pathological injury occurred in the alveolar septal area of the formalin rat lungs.

3.1.3 Proteomics

Because our interest was mainly in that subset of proteins whose expression was altered by formalin exposure and whose expression was normalized by substance P pretreatment, a total of 71 protein spots, including the spots from the statistical tests and the unique pattern changes, were cut for identification by peptide mass fingerprinting and LC-MS/MS.

One population of proteins included those down-regulated by formalin treatment, an alteration prevented by pretreatment with SPa. Twenty-one of the 71 proteins fell into this category, but many of them were fairly low in abundance. Only nine of the 21 had a detectable abundance of 200 PPM or greater (Figure 2a). Eight of the 21 spots were

rendered undetectable by formalin treatment, reappearing with the SPa treatment (SSP 8516, 1604, 8523, 8507, 1302, 2320, 8303, and 8203; Table 3). In addition, five of the 71 spots appeared in the SPa group only, but their intensities were well below 200 PPM and therefore not identifiable by mass spectrometry.

Another interesting subset of proteins were those up-regulated by formalin treatment, a change prevented by SPa pretreatment. Twenty-three of the 71 spots were classified in this category. Half of these proteins were unidentifiable (Figure 2b). An example of protein expression changes (Figure 3) is a spot (SSP 5711, identified as selenium binding protein 2) that had shifted, but the spot position was slightly ambiguous in the control group. In the formalin treated, the spot was more acidic, while in the SPa treated group the spot was more basic.

Peptide mass fingerprint and LC-MS/MS analysis of protein cutouts identified proteins whose expression was significantly altered as determined by 2-DE (Tables 3-6). Although these alterations in protein abundance were statistically significant based on ANOVA, the brief time duration suggests they were the result of differential post-translational modification, and not necessarily up- or down-regulation of expression. However, changes in protein levels for several nuclear proteins functioning in transcription regulation were noted (Table 7).

One of the more prominent and unique effects of formalin exposure and substance P pretreatment that were probably unrelated to altered post-translational modification during the 43 minute post-exposure period was our observation of significant alterations in the expression of alpha and beta fibrinogen subunits. Formalin had little consistent effect on lung fibrinogen, while the substance P pretreatment changed the type of fibrinogen found in the lung tissue (Figure 4). Alpha fibrinogen was induced by SPa pretreatment. Beta fibrinogen seems to have undergone a mass increase and an apparent increase in abundance with SPa.

3.1.4 Bioinformatics

We were interested in knowing if these identified proteins were uniformly expressed in homogenized lung tissue to provide further evidence that our MS identification techniques were valid and that our tissue preparation was adequate. A detailed search of GEO profiles (Gene Expression Omnibus) at the NCBI website was done (http://www.ncbi.nlm.nih.gov/sites/entrez). Three separate studies were referenced to confirm gene expression in homogenized lung, and in many cases the directional change in gene expression was congruent with our proteomic findings. All the identified proteins were found to have some level of gene expression in homogenized lung [8-10].

An IPA ontological analysis of the entire population of differentially-expressed proteins revealed that the primary groupings were associated with cell signaling, cell death with a focus on apoptosis, and tumorigenesis (Table 8). The top three canonical pathways represented in the differentially expressed proteins are involved in cellular signaling - Acute Phase Response Signaling, NRF-2 Mediated Oxidative Stress Response, and Cell Cycle: G2/M DNA Damage Checkpoint Regulation (Table 9). The top function for the most significant network for both formalin and SPa is embryonic development. The other top four networks involve cell death, inflammatory disease, cell to cell signaling, and post-translational modification (Table 10).

3.1.5 Discussion

The results demonstrate pulmonary function and proteomic changes consistent with formalin exposure-related injury. They also demonstrate a significant effect on the injury-related proteome of rats that were pretreated with an aerosolized substance P analog, which has been shown in previous studies to protect pulmonary tissue from toxic damage [11,12]. Perhaps some of these protein changes can explain the protective effects of substance P.

Substance P is a tachykinin ($C_{63}H_{98}N_{18}O_{13}S$) which has numerous physiological roles in the body. Tachykinins are active peptides which excite neurons, evoke behavioral responses, potently vasodilate, act as secretagogues, and contract (directly or indirectly) many smooth muscles [13]. In the human lung there are few substance P secretory neurons, however, macrophages are known to synthesize and release SP. Thus, it is thought that macrophages may be responsible for producing most of the SP found in lung tissue [14-16]. The molecular mechanisms of substance P's action in the pulmonary tissue are an area of active research.

At other physiologic sites, SP may cause plasma extravasation via upregulation of integrins and intracellular adhesion molecules on both endothelial cells and migrating leukocytes [17]. The upregulation of these adhesion molecules is mediated by NK1 receptors found on both endothelial cells and leukocytes. Recent findings suggest that substance P binds to the NK1 receptor on cells of the immune system. *In vitro* studies have shown that SP can act as a chemoattractant for both neutrophils and eosinophils [18]. In the CNS substance P has a role in behavior, pain transmission, and emesis.

In this study, brief but intense formalin exposure caused a 33-fold increase in inspiratory lung compliance. Changes in inspiratory dynamic lung compliance are typically associated with chronic lung disease and accompanying pathological changes in the small airways [19]. Most of the pathological injury observed here occurred in the alveolar septal area and adjacent terminal bronchioles of the formalin rat lungs. This strongly suggests that the 33-fold increase in inspiratory dynamic lung compliance in the formalin rat group –vs- the formalin + SPa group rats is associated with a formalin-induced combination of structural/neural changes.

A >6 fold increase in lung permeability was also observed. The damaged alveolar-capillary membranes are consistent with the increase in lung permeability as measured by the increase in 99mTc-DTPA clearance in the formalin rats –vs- the formalin + Sar^{9}, Met $(O_2)^{11}$-substance P analog treated group. This is also consistent with a prior study of toxic exposure in cell lines [12]. In that study administered ozone resulted in a dose dependent increase in barrier permeability in canine bronchial epithelial cells as measured by mannitol flux. The addition of SP alone had no affect on bronchial epithelial permeability but it inhibited the permeability-enhancing effect of ozone. This protective effect of SP was sustained for 2 hours after ozone exposure. It was also noted that the substance P analog ASMSP (acetyl-[Arg6,Sar9,Met(O2)11]-SP(6-11)), which is similar to SPa used in the present study, prevented ozone induced lung permeability changes [12].

Proteins whose expression decreased following formalin exposure may either be post-translationally modified forms (charge variants) that are modified to a lesser extent, or previously unmodified forms that are now modified. The converse also applies to proteins whose abundance increased. However, protein levels of CNOT8, which is

associated with post-translational modifications (Table 8), such as the methylation of substrates for protein arginine methyltransferase 1 [20], and is a ubiquitous transcription factor associated with RNA polymerase II transcription generally functioning as a negative regulator of cell proliferation [21], were elevated 31.4-fold by formalin exposure, but maintained near control levels by pre-treatment with SPa (Table 7). Additionally, protein arginine methyltransferase 2 was down-regulated 46.83-fold. Two other proteins functioning in transcription regulation, Hmgb4 and ZNF354a, demonstrated no changes in the formalin group, but had greatly elevated levels in the SPa pretreatment group (Table 7). ZNF354a is thought to contribute to changes in rRNA synthesis and its up-regulation to be associated with a general increase in cellular activity [22].

The top three canonical pathways were associated with cellular signaling involving acute phase response signaling, NRF-2 mediated oxidative stress response, and cell cycle specific to the G2/M DNA damage checkpoint regulation. The primary ontological groupings and networks were also associated with cellular signaling and cell death (focused on apoptosis).

The changes in the Acute Phase Response Signaling Pathway associated with formalin exposure demonstrated changes consistent with lung pathology. However, greater changes were demonstrated in the levels of fibrinogen (Table 7) after SPa + formalin exposure, and this group experiences no associated alterations in lung function as measured by lung permeability or inspiratory dynamic lung compliance (Tables 1 & 2). The 2-DE gels demonstrated prominent changes in fibrinogen subunits. Fibrinogen has been shown to be expressed in lung epithelial cells, and to be physiologically induced by inflammatory events [23]. Formalin had no consistent affect on alpha or beta fibrinogen (Figure 4) while SPa pretreatment altered both subunits. Alpha fibrinogen (FBG) was highly abundant with SPa, whereas in the control and formalin groups it was not detected. Beta FBG has been identified by multiple MS studies in our laboratory indicating an increase in mass and concentration with SPa pretreatment. We believe these 2-DE findings for FBG subunits reflect pulmonary tissue protein changes, as opposed to a vascular source. Albumin abundance is low and consistent across all samples, showing that the tissues were adequately saline-perfused prior to solubilization.

In previous studies, cultured human pulmonary epithelial cell lines (A459) have been shown to produce and secrete intact FBG upon stimulation with inflammatory mediators [24]. This secretion mostly occurs basolaterally. In an unstimulated state mRNA for the gamma FBG chain is detectable but not for alpha and beta FBG [23]. Our findings support the belief that alpha chain is not produced constitutively, as seen in the controls in figure 4. It is noted that formalin alone does not seem to stimulate alpha chain production in this 42 minute time frame. However, SPa pretreatment (group SP) causes a consistently significant increase in alpha chain production. We postulate that this is produced by lung epithelial cells in response to substance P analog stimulation. Perhaps this is mediated through an interleukin, as it has been shown that SP can stimulate NK-1 receptors which activate NF-kappa B, a transcription factor which controls expression of many cytokines such as interleukin-8 [25].

A hallmark of acute respiratory distress syndrome is fibrin deposition in the lungs. Perhaps this fibrin is derived from alveolar epithelial cells. This study suggests that

subunit expression by lung tissue can be altered by an aerosolized substance P analog. Current ideas on alveolar fibrin deposition revolve around various procoagulant factors vs. fibrinolytic factors. For example, increased levels of tissue factor mRNA and plasminogen activator – inhibitor (PA-I) mRNA as well as a reduction in PA mRNA gene expression occurs in rodent ARDS models after pulmonary insult [26]. This creates a mismatch between procoagulant factors and fibrinolytic factors, with the balance in favor of fibrin deposition. In severe ARDS, a persistent alveolar fibrin layer may provide a matrix for macrophage migration and promotes angiogenesis and collagen deposition [26]. We are suggesting that this fibrin may be actively secreted by lung epithelial cells as intact fibrinogen into the alveoli. It would augment any FBG that has leaked from the vasculature. In our model we have shown that substance P is protective against acute toxin exposure, but in the ARDS model substance P could be inducing FBG production by lung tissue and adding to the pathologic state. The elevated levels of fibrinogen alpha associated with SPa pretreatment have been linked in a cell to cell signaling network with decreased levels of Septin-9 and cathepsin A (Table 10). Cathepsin A is a protective protein which appears to be essential for both the activity of beta-galactosidase and neuraminidase. Cathepsin A is also a carboxypeptidase and can deamidate tachykinins. Cathepsin A protein was elevated 1.40-fold in the formalin exposure and decreased 4.48-fold by the analog of the tachykinin Substance P.

Additionally, SPa network 2 associated with inflammatory disease (Table 10) suggests that the elevated levels of vimentin (Table 7) may be associated with inflammation induced by SPa + formalin exposure, but not with formalin alone. Along with actin and tubulins, vimenten is a third class of well-characterized cytoskeletal elements associated specifically with mesenchymal tissues. Vimentin has been implicated as an autoantigen in pulmonary inflammation and bound to HLA-DR presented by human brochoalveolar lavage cells in patients with sarcoidosis, an inflammatory disease which is often located in the lungs [27,28].

Cell signaling in the NRF-2 Mediated Oxidative Stress Response Pathway and cell cycle G2/M DNA damage checkpoint regulation both involve the 519-fold decrease in the ubiquitin B protein (UBB). Ubiquitin B is a protein modifier which can be covalently attached to target lysines as a lysine-linked polymer leading to their degradation by proteasome. Attachment to proteins as a monomer or as an alternatively linked polymer does not lead to degradation and may be required for cellular processes such as the cell cycle and cell death [29], regulation of gene expression, stress response, ribosome biogenesis, DNA repair, and maintenance of chromatin structure. A specific role for ubiquitin which may be applicable in explaining the SPa prevention of the formalin-induced combination of structural/neural changes, is the prominent role ubiquitin plays in the formation and function of neural circuits [30]. UBB may be the central actor in mediating the SPa-associated prevention of formalin-induced acute lung injury.

Acute Respiratory Distress Syndrome (ARDS) is usually associated with vascular permeability and edema. Epithelial sodium channels (ENaC) play a critical role in reestablishing salt and fluid homeostasis in ARDS. Possession of an abnormal number of channels is associated with pathological pulmonary conditions, such as cystic fibrosis [31]. These sodium channels have a high turn-over rate, a half-life of about 1 hour, are targeted for degradation by the ubiquitin-protein ligase Nedd4 [32] and are postulated to be generally regulated by ubiquitination[33]. The greater the number of channels

available to restore homeostasis, the less time spent in an edema formation state. The SPa-treatment was associated with a 519-fold decrease in levels of ubiquitin B (Table 7) and the reappearance of the sodium channel beta 3 subunit (Table 4).

The remainder of the discussion will focus on highly relevant proteins that were observed to be altered with formalin exposure, but do not fall into an IPA canonical pathway. These proteins are spectrin (alpha chain), peroxiredoxin 1, ATP synthase beta subunit, hyaluronoglucosaminidase 3, glyceraldehyde-3-phosphate dehydrogenase, annexin 1, BCL-2, cytokeratin-8 and 19.

Spectrin alpha chain is a cytoskeletal protein involved in maintaining cell shape, polarity, and membrane structure. In a study by Lee, et al, fragmentation of spectrin by caspase results in reduced membrane association and thus may lead to permanent remodeling of the membrane skeleton of the chick lens [34]. Spectrin is important for maintaining cell membrane integrity and formalin may exhibit toxicity by either down regulating spectrin or chemically modifying this important protein.

Peroxiredoxin 1 (Prdx1) is a well known protein with antioxidant effects. We have previously shown peroxiredoxin 2, which is structurally similar to Prdx1, to be down regulated by certain jet fuel (JP-8) exposures in mice [35]. Peroxiredoxin 1 catalyzes the removal of thiyl radicals before they generate more reactive radicals and cause oxidative damage to biomolecules. The decline in this enzyme could increase oxidative damage caused by inhaled toxins. More studies of peroxiredoxin isoforms needs to be done to determine the effect that toxins have on this proteins function and expression. Some studies have shown that Prdx1mRNA expression increases with toxin exposure [10]. In the present study, the decrease in Prdx1 observed in formalin exposure and over-compensation with SPa in this putative charge variant suggests alterations in the level of post-translational modification after 42 minutes.

Hyaluronoglucosaminidase 3 is decreased by formalin and preserved by SPa pretreatment. Hyaluronoglucosaminidase 3 degrades hyaluronan, a linear polysaccharide which is accumulated in lung interstitium during different pathological conditions, causing interstitial edema and thereby impaired lung function [36]. In another study prolonged exposure of rats to cigarette smoke resulted in significant alteration in the metabolism of glycosaminoglycans (GAG) and glycoproteins (GP). In the lungs glycosaminoglycans (including hyaluronan) increased with cigarette smoke exposure, which appears to be due to decreased hyaluronoglucosamindase activity [37]. Formalin decreases the abundance of this enzyme, suggesting a mechanism whereby formalin may cause pulmonary interstitial edema and impaired lung function.

Glyceraldehyde-3-phospate dehydrogenase (GAPDH) is an enzyme of the glycolytic pathway. In our study it is decreased by formalin. Interestingly, a similar proteomic study has shown this enzyme to increase after formalin exposure [38]. Our study was an acute, high dose exposure, while the previous study was a fifteen day exposure study, perhaps explaining the discrepancy. The loss or downregulation of GAPDH could have devastating effects on energy production and defense from oxidative stress, as described by Yang, *et al.*

Several proteins involved in cell death were noted. Two notable proteins were decreased in formalin exposed groups but were preserved by SPa; annexin 1 and BCL-2. Annexin 1 is a well known protein with anti-inflammatory effects, primarily by decreasing white blood cell extravasation into inflamed tissue. Other evidence suggests

annexin 1 causes apoptosis of neutrophils in a timely manner at the site of inflammation, and therefore decreases the inflammatory process to pulmonary insults [39]. When this protein is neutralized or down regulated by formalin, local inflammation and toxicity can occur. Annexin 1 is also responsible for membrane fusion and exocytosis and its absence may interfere with surfactant release. BCL-2 is an anti-apoptotic protein which is well known in cancer literature. In our study this protein was identified by 2-D electrophoresis. The fact that BCL-2 decreases in formalin exposure is consistent with toxicity. A recent paper has shown that ubiquitination of BCL-2 and proteosomal degradation causes apoptosis [40].

Cytokeratin-8 expression has been shown to be altered by cigarette exposure [41]. The bronchus of rats exposed to smoke for eight days has yielded altered levels of cytokeratin-8. These findings indicate that changes in cytokeratin expression in respiratory tract epithelial cells are a sensitive marker for a cellular stress response. A detailed human study of acute lung injury patients has shown high cytokeratin-19 fragments in the pulmonary lavage fluid of affected patients. Higher levels of the CK-19 fragments indicated a poor prognosis [42]. In our study both of these keratins were increased by formalin, an effect prevented by SPa pretreatment.

In conclusion, we sought to determine if substance P analog pretreatment would attenuate protein alterations and pulmonary function abnormalities associated with formalin-induced lung injury. An impressive deterioration in pulmonary function with formalin inhalation was blocked by pretreatment with substance P. Histologic damage was noted with the formalin only group, and SPa prevented these changes. In this study, proteomic techniques were useful for demonstrating molecular changes associated with a substance P analog pretreatment. The SP analog altered the injury-related proteome of rats exposed to aerosolized formalin, with cytoskeletal markers of damage such as cytokeratin-8 and 19 being preserved at normal levels. Fibrinogen subunit expression was altered by substance P pretreatment and we believe this is a novel finding for this *in vivo* model. This rodent model for inhalation injury has shed light on the protective effects of substance P on the chemically-exposed lung.

3.2 JP-8 effects on Type II Alveolar Cells *in vitro*.

This portion of our project was undertaken to assess the effect of JP-8 exposure on rat alveolar type II epithelial cells, at sub lethal levels that are occupationally relevant. An equally important aim was to assess the utility of a novel gel-free/label-free proteomics approach to quantify JP-8-mediated alterations in cellular protein expression. Alveolar type II cells (1×10^6 cells/well) were cultured in 6-well plates and exposed to JP-8 jet fuel (0.1 µg/mL, 0.4 µg/mL, 2.0 µg/mL, vehicle control, and media control) for 1 and 6 h. Cells from each of 6 wells per treatment group (n=6) were solubilized in situ and proteins trypsinized. Tryptic peptides from each sample were analyzed serially via linear ion-trap LC-MS/MS. Proteins were identified using SEQUEST and X!Tandem while protein quantification was carried out based on total ion chromatograms using the proprietary technology of Indiana Centers for Applied Protein Sciences (INCAPS). In this approach, the integral volume under each selected peptide peak was measured, normalized, and compared for relative abundance.

3.2.1 Summary of Results.

1. Nitric Oxide production was increased by JP-8 in both 1 h and 6 h exposures; Cell viability was unaffected by 1 h JP-8 exposure; 0 viability at 6 h, 2.0 µg/mL (see Figure 5).
2. 2,461 proteins were identified and quantified. Of these, 611 proteins were identified with high confidence and another 658 proteins were categorized as Priority 2.
3. Of these 1,269 proteins, 608 proteins had at least one significant change between groups. The sample median % Coefficient of Variation (%CV) for the Priority 1 proteins was 9.09%.
4. General group comparisons are presented in Tables 11-14 in the Appendix.

3.2.3 Conclusions.

1. In this experiment, *in vitro* JP-8 jet fuel exposure, at a level considered to be low (≤2 µg/mL), reduced rat AEII cell viability to 0% after only 6 h, whereas 1 h of exposure had little effect in this regard.

2. In contrast, both exposure durations increased NO production, an injury response that was more extensive at 6 h.

3. The 6 h exposure, at 2 µg/mL resulted in down-regulation of 90% of the proteins altered by ≥ 1.5-fold as determined by quantitative mass spectrometry. Culture duration had little effect on protein expression in unexposed controls.

4. Decreased cell viability corresponded to significant down-regulation of proteins involved in all manner of cell activity, but predominantly via decreased translational and protein synthetic machinery (See Figures 6 and 7).

These results are very consistent with the gene expression alterations (as measured by microarray) in mice exposed for 1 h to 1000 mg/m^3 JP-8 and organs sampled at 6 h by David T. Harris at Univ. of Arizona. He concluded that JP-8 exposure induces the loss of both 18S and 28S RNA in exposed cells (due to loss of ribosomal proteins) that occurs between 6 and 24 hours after in vivo exposure.

3.3 Carbon nanoparticle effects *in vitro* on protein expression and function in murine kidney epithelial cells

In our transition/expansion to nanotoxicology and the application of our proteomics platform to this additional area of AFOSR interest, we have developed a new collaboration with Dr. Bonnie Blazer-Yost in the IUPUI Dept. of Biology to assess carbon nanoparticle (CNP) exposure effects on barrier epithelia.

3.3.1 Introduction

Carbon nanoparticles (CNP) are currently used in many industries, and their future application is likely to increase. Three common types include single wall carbon nanotubes (SWCNT), multiwall carbon nanotubes (MWCNT), and fullerenes (C_{60}). SWCNT consist of covalently bound carbon atoms arranged in a long, thin tube-like structure with a diameter of approximately 1.4 nm [43]. MWCNT have a similar structure, but they are longer than SWCNT and consist of several complex layers of nanotubes inside each other with a diameter of 10-20 nm [43]. C_{60} consist of 60 carbon

atoms covalently linked together to form a spherical molecule.

Recent research has revealed diverse effects of CNPs on biological systems. One study indicated that SWCNT and MWCNT inhibit growth by apoptosis and loss of cell adhesion [44], while other studies suggest that carbon nanotubes seem to increase the growth of mesenchymal cells, cause fibrogenesis, and cause granuloma formation [45]. We have previously shown that MWCNT alter expression of genes for cellular transport, metabolism, cell cycle regulation, and stress response [46]. MWCNT are of special interest because of their structural similarity to asbestos [47]. Early experiments with fullerenes have shown them to be cytotoxic, and they have been shown to bind to ion channels [48]. Various types of nanoparticles are endocytosed and can alter the cytoskeletal organization [49].

The cell model used in the current study is the mouse principal cell type of the kidney cortical collecting duct, clone 4 ($mpkCCD_{cl4}$) cell line. $mpkCCD_{cl4}$ cells grow to form a confluent monolayer that simulates the barrier epithelial function and hormone responsiveness found in vivo in renal collecting ducts. These cells are of particular interest because they are responsible for much of the hormonally-regulated ion transport in the kidney. If the CNP exposure alters these cells, salt homeostasis could be modulated, resulting in changes in blood pressure.

We hypothesized that CNP exposure alters $mpkCCD_{cl4}$ cells resulting in abnormal cellular function. Experiments were conducted to determine functional, structural and proteomic changes induced by application of CNP to the renal barrier epithelial cells. Electrophysiological studies were used to determine the effect of CNPs on transepithelial electrical resistance (TEER). Imaging studies were conducted to observe changes in specific cytoskeletal components and nuclear proliferation. Quantitative proteomic studies were conducted to correlate the observed structural and functional studies with CNP-induced changes in the expressed cellular proteome.

3.3.2 Results

A 48 hour exposure to 20 $\mu g/cm^2$ of either sonication suspended SWCNT or MWCNT significantly decreased the transepithelial resistance of the cellular monolayer (Figure 8). At this concentration, C_{60} had no significant effect.

Imaging studies revealed that CNP prepared by sonication and applied at a concentration of 20 µg/ml for 48 hours tended to agglomerate before settling on the monolayer. PCNA imaging showed that MWCNT and SWCNT agglomeration induced nuclear proliferation in cells surrounding the agglomerations (Figure 9, top). In a separate experiment, an increase in actin filaments was seen in cells surrounding agglomerations. Chronic, low-level exposure to MWCNT and SWCNT (5 $\mu g/cm^2$ thrice weekly) induced an increased number and size of large multi-nucleated cells. Staining with rhodamine-phalloidin also revealed a general increase in expression of polymerized actin.

Differential protein expression at high dose SWCNT and MWCNT exposures determined by 2-DE is shown in Table 16. The expression of 11 proteins deemed either directly or indirectly associated with cell proliferation and function were altered by exposure. LFQMS analysis of CNP exposure for 48 h resulted in differential expression (via ANOVA) of 43 proteins variably effected by the different CNPs. Those whose expression differed from control are listed in Table 17.

3.3.3 Discussion

The electrophysiological studies and imaging studies indicate changes in cell function in cells treated with CNP. To more closely model *in vivo* exposures, functional changes were measured in mpkCCD$_{cl4}$ cells treated with CNP suspended via sonication. Previous studies have indicated that coated nanoparticles remain in solution, while unaltered nanoparticles agglomerate and settle out of solution. In the present study, visual observation confirmed that sonication increased the solubility and decreased agglomerate particle size although there is still a degree of agglomeration and precipitation onto the cellular monolayer.

TEER is a measure of monolayer integrity and is also a very sensitive measure of cellular viability. As cellular viability decreases, TEER falls precipitously. In the experiments shown in Figure 1, the decrease in TEER is substantial after treatment with either single- or multi-wall carbon nanotubes. However, these changes do not represent a decrease in cell viability. Control monolayers had an average TEER of 2370 ± 815 $\Omega \cdot cm^2$. A decrease to 1477 $\pm$ 530 (SWCNT treated) or 1274 $\pm$ 465 (MWCNT treated) still exceed 1000 $\Omega \cdot cm^2$ which is considered a high resistance, intact epithelium. The changes in resistance indicate more subtle changes within the cells. Examples of cellular alterations which could be manifested as changes like these would be minor modifications of the cytoskeleton which is a major component in determining the impermeability of the junctional complexes or changes in the composition of the cellular membrane which would be sufficient to alter permeability.

Studies have suggested that CNP may have carcinogenic properties [50]. MWCNT have been specifically implicated due to their structural similarity to chrysotile asbestos that is widely accepted to cause carcinogenic responses in humans. After acute exposure to MWCNT and SWCNT, we observed changes in cells surrounding agglomerations of SWCNT and MWCNT. Cells seemed to exhibit proliferating nuclei as indicated by PCNA staining. In normal cells, once confluence is reached, cells no longer actively divide. These results indicate that SWCNT and MWCNT agglomerations cause cells to replicate abnormally, suggesting possible carcinogenic properties. Chronic treatment with CNP (especially MWCNT) suspended via sonication also revealed an increased number of large, multinucleated cells. Polyploidy, as observed here, is an indicator of genotoxicity and suggests that CNP (at these exposure levels) may be mutagenic.

mpkCCD$_{cl4}$ cells treated acutely with SWCNT and MWCNT as well as cells treated chronically with any of the three CNP types seemed to exhibit an increased expression of actin filaments. Previously, such changes in actin expression have contributed to a decrease in cell viability [51]. Our observed trends in cell function and abnormal nuclear proliferation seen via PCNA staining, support this. However, the proteomic results do not support differential expression of total actin. Taken together, these results suggest that the changes we have observed in the filamentous (phalloidin-stained) actin are the result of changes in the filamentous/globular actin ratio in the cells.

Conclusion. The present study has shown that CNP induced significant alterations in renal collecting duct cell function, histology, and protein expression. CNP suspended via sonication cause histological changes including increased nuclear proliferation, elevated filamentous actin expression, and multinucleation. The observed changes are subtle

and likely represent cellular alterations that would have physiological effects over a prolonged time-course.

4 References

1. Witten M, Robledo R: **NK1-receptor activation prevents hydrocarbon-induced lung injury in mice**. *Am J Physiol.* 1999, **276**:L229-238.
2. Rodarte JR, Rehder K: **Dynamics of respiration**. In *Handbook of Physiology: The Respiratory System.* Edited by: Am. Physiol. Soc.; 1986:131-144. vol III.]
3. Wang S, Young RS, Sun NN, Witten ML: **In vitro cytokine release from rat type II pneumocytes and alveolar macrophages following exposure to JP-8 jet fuel in co-culture**. *Toxicology* 2002, **173**:211-219.
4. Kaplan RS, Pedersen PL: **Determination of microgram quantities of protein in the presence of milligram levels of lipid with amido black 10B**. *Anal Biochem* 1985, **150**:97-104.
5. Higgs RE, Knierman MD, Gelfanova V, Butler JP, Hale JE: **Comprehensive label-free method for the relative quantification of proteins from biological samples**. *J Proteome Res* 2005, **4**:1442-1450.
6. Higgs RE, Knierman MD, Gelfanova V, Butler JP, Hale JE: **Label-free LC-MS method for the identification of biomarkers**. *Methods Mol Biol* 2008, **428**:209-230.
7. Wang M, You J, Bemis KG, Tegeler TJ, Brown DPG: **Label-free mass spectrometry-based protein quantification technologies in proteomic analysis**. *Brief Funct Genomic Proteomic* 2008, **7**:329-339.
8. Dillman JF, Phillips CS, Dorsch LM, Croxton MD, Hege AI, Sylvester AJ, Moran TS, Sciuto AM: **Genomic analysis of rodent pulmonary tissue following bis-(2-chloroethyl) sulfide exposure.** *Chem Res Toxicol.* 2005, **18** 28-34.
9. Lee CT, Ylostalo J, Friedman M, Hoyle GW: **Gene expression profiling in mouse lung following polymeric hexamethylene diisocyanate exposure**. *Toxicol Appl Pharmacol* 2005, **205**:53-64.
10. Sciuto AM, Phillips CS, Orzolek LD, Hege AI, Moran TS, Dillman JF: **Genomic analysis of murine pulmonary tissue following carbonyl chloride inhalation**. *Chem Res Toxicol* 2005, **18**:1654-1660.
11. Prior M, Green F, Lopez A, Balu A, DeSanctis GT, Fick G: **Capsaicin pretreatment modifies hydrogen sulphide-induced pulmonary injury in rats**. *Toxicol Pathol.* 1990, **18**:279-288.
12. Yu XY, Undem BJ, Spannhake EW: **Protective effect of substance P on permeability of airway epithelial cells in culture**. *Am J Physiol* 1996, **271**:L889-895.
13. Uniprot: **Uniprot online database**. Edited by; 2006.
14. Bost KL, Breeding SA, Pascual DW: **Modulation of the mRNAs encoding substance P and its receptor in rat macrophages by LPS**. *Reg Immunol* 1992, **4**:105-112.
15. Ho WZ, Lai JP, Zhu XH, Uvaydova M, Douglas SD: **Human monocytes and macrophages express substance P and neurokinin-1 receptor**. *J Immunol* 1997, **159**:5654-5660.

16. Killingsworth CR, Shore SA, Alessandrini F, Dey RD, Paulauskis JD: **Rat alveolar macrophages express preprotachykinin gene-I mRNA-encoding tachykinins**. *Am J Physiol* 1997, **273**:L1073-1081.
17. Geppetti P, Holzer P: In *Neurogenic Inflammation*. Edited by Geppetti P, Holzer P: CRC Press; 1996.
18. Roch-Arveiller M, Regoli D, al. e: **Tachykinins: effects on motility and metabolism of rat polymorphonuclear leucocytes**. *Pharmacology* 1986, **33**:266-273.
19. Comroe JH, Forster RE, Dubois AB, Briscoe WA, Carlsen E: *The Lung*. Chicago: Yearbook Publishers; 1962.
20. Robin-Lespinasse Y, Sentis S, Kolytcheff C, Rostan MC, Corbo L, Le Romancer M: **hCAF1, a new regulator of PRMT1-dependent arginine methylation**. *J Cell Sci* 2007, **120**:638-647.
21. Bogdan JA, Adams-Burton C, Pedicord DL, Sukovich DA, Benfield PA, Corjay MH, Stoltenborg JK, Dicker IB: **Human carbon catabolite repressor protein (CCR4)-associative factor 1: cloning, expression and characterization of its interaction with the B-cell translocation protein BTG1**. *Biochem J* 1998, **336**:471-481.
22. Shakib K, Norman JT, Fine LG, Brown LR, Godovac-Zimmermann J: **Proteomics profiling of nuclear proteins for kidney fibroblasts suggests hypoxia, meiosis, and cancer may meet in the nucleus**. *Proteomics* 2005, **5**:2819-2838.
23. Simpson-Haidaris P: **Induction of fibrinogen biosynthesis and secretion from cultured pulmonary epithelial cells**. *Blood*. 1997, **89**:873-882.
24. Guadiz G SL, Goss RA, Lawrence SO, Marder VJ, Simpson-Haidaris PJ: **Polarized Secretion of Fibrinogen by Lung Epithelial Cells** *Am J Respir Cell Mol Biol.* 1997, **17**:60-69.
25. Williams R, Zou X, Hoyle G: **Tachykinin-1 receptor stimulates proinflammatory gene expression in lung epithelial cells through activation of NF-kappaB via a G(q)-dependent pathway**. *Am J Physiol Lung Cell Mol Physiol.* 2007, **292**:430-437.
26. Fan J, Kapus A, Li Y, Rizoli S, Marshall J, Rotstein O: **Priming for Enhanced Alveolar Fibrin Deposition after Hemorrhagic Shock: Role of Tumor Necrosis Factor**. *Am. J. Respir. Cell Mol. Biol.* 2000, **22**:412-421.
27. Wahlstrom J, Dengjel J, Persson B, Duyar H, Rammensee HG, Stevanovic S, Eklund A, Weissert R, Grunewald J: **Identification of HLA-DR-bound peptides presented by human bronchoalveolar lavage cells in sarcoidosis**. *J Clin Invest* 2007, **117**:3576-3582.
28. Yang Y, Fujita J, Bandoh S, Ohtsuki Y, Yamadori I, Yoshinouchi T, Ishida T: **Detection of antivimentin antibody in sera of patients with idiopathic pulmonary fibrosis and non-specific interstitial pneumonia**. *Clin Exp Immunol* 2002, **128**:169-174.
29. Joazeiro CA, Weissman AM: **RING finger proteins: mediators of ubiquitin ligase activity**. *Cell* 2000, **102**:549-552.
30. Murphey RK, Godenschwege TA: **New roles for ubiquitin in the assembly and function of neuronal circuits**. *Neuron* 2002, **36**:5-8.

31. Stutts MJ, Canessa CM, Olsen JC, Hamrick M, Cohn JA, Rossier BC, Boucher RC: **CFTR as a cAMP-dependent regulator of sodium channels**. *Science* 1995, **269**:847-850.
32. Staub O, Dho S, Henry P, Correa J, Ishikawa T, McGlade J, Rotin D: **WW domains of Nedd4 bind to the proline-rich PY motifs in the epithelial Na+ channel deleted in Liddle's syndrome**. *Embo J* 1996, **15**:2371-2380.
33. Staub O, Gautschi I, Ishikawa T, Breitschopf K, Ciechanover A, Schild L, Rotin D: **Regulation of stability and function of the epithelial Na+ channel (ENaC) by ubiquitination**. *Embo J* 1997, **16**:6325-6336.
34. Lee A, Morrow J, Fowler V: **Caspase remodeling of the spectrin membrane skeleton during lens development and aging.** *J Biol Chem.* 2001 **276**:20,735-742.
35. Witten M, Witzmann F, Bauer M, Fieno A, Grant R, Keough T, Kornguth S, Lacey M, Siegel F, Sun Y, et al.: **Proteomic analysis of simulated occupational jet fuel exposure in the lung**. *Electrophoresis* 1999, **20**:3659-3669.
36. Teder P, Heldin P: **Mechanism of impaired local hyaluronan turnover in bleomycin-induced lung injury in rat.** *Am J Respir Cell Mol Biol.* 1997, **17**:376-385.
37. Latha M, Vijayammal P, Kurup P: **Changes in the glycosaminoglycans and glycoproteins in the tissues in rats exposed to cigarette smoke.** *Atherosclerosis.* 1991 **86**:49-54.
38. Yang YH, Xi ZG, Chao FH, Yang DF: **Effects of formaldehyde inhalation on lung of rats**. *Biomed Environ Sci* 2005, **18**:164-168.
39. Solito E, Kamal A, Russo-Marie F, Buckingham JC, Marullo S, Perretti M: **A novel calcium-dependent proapoptotic effect of annexin 1 on human neutrophils**. *FASEB J* 2003, **17**:1544-1546.
40. Chanvorachote P, Nimmannit U, Stehlik C, Wang L, Jiang BH, Ongpipatanakul B, Rojanasakul Y: **Nitric oxide regulates cell sensitivity to cisplatin-induced apoptosis through S-nitrosylation and inhibition of Bcl-2 ubiquitination**. *Cancer Res* 2006, **66**:6353-6360.
41. Schlage WK, Bulles H, Friedrichs D, Kuhn M, Teredesai A, Terpstra PM: **Cytokeratin expression patterns in the rat respiratory tract as markers of epithelial differentiation in inhalation toxicology. II. Changes in cytokeratin expression patterns following 8-day exposure to room-aged cigarette sidestream smoke**. *Toxicol Pathol* 1998, **26**:344-360.
42. Stern JB, Paugam C, Validire P, Adle-Biassette H, Jaffre S, Dehoux M, Crestani B: **Cytokeratin 19 fragments in patients with acute lung injury: a preliminary observation**. *Intensive Care Med* 2006, **32**:910-914.
43. Jia G, Wang H, Yan L, Wang X, Pei R, Yan T, Zhao Y, Guo X: **Cytotoxicity of carbon nanomaterials: single-wall nanotube, multi-wall nanotube, and fullerene**. *Environ Sci Technol* 2005, **39**:1378-1383.
44. Cui DX, Tian FR, Ozkan CS, Wang M, Gao HJ: **Effect of single wall carbon nanotubes on human HEK293 cells**. *Toxicology Letters* 2005, **155**:73-85.
45. Donaldson K, Aitken R, Tran L, Stone V, Duffin R, Forrest G, Alexander A: **Carbon nanotubes: a review of their properties in relation to pulmonary toxicology and workplace safety**. *Toxicol Sci* 2006, **92**:5-22.

46. Witzmann FA, Monteiro-Riviere NA: **Multi-walled carbon nanotube exposure alters protein expression in human keratinocytes**. *Nanomedicine* 2006, **2**:158-168.
47. Poland CA, Duffin R, Kinloch I, Maynard A, Wallace WAH, Seaton A, Stone V, Brown S, MacNee W, Donaldson K: **Carbon nanotubes introduced into the abdominal cavity of mice show asbestos-like pathogenicity in a pilot study**. *Nat Nano* 2008, **3**:423-428.
48. Park KH, Chhowalla M, Iqbal Z, Sesti F: **Single-walled carbon nanotubes are a new class of ion channel blockers**. *J Biol Chem* 2003, **278**:50212-50216.
49. Gupta AK, Gupta M: **Cytotoxicity suppression and cellular uptake enhancement of surface modified magnetic nanoparticles**. *Biomaterials* 2005, **26**:1565-1573.
50. Murr LE, Garza KM, Soto KF, Carrasco A, Powell TG, Ramirez DA, Guerrero PA, Lopez DA, Venzor J, 3rd: **Cytotoxicity assessment of some carbon nanotubes and related carbon nanoparticle aggregates and the implications for anthropogenic carbon nanotube aggregates in the environment**. *Int J Environ Res Public Health* 2005, **2**:31-42.
51. Shvedova AA, Castranova V, Kisin ER, Schwegler-Berry D, Murray AR, Gandelsman VZ, Maynard A, Baron P: **Exposure to carbon nanotube material: assessment of nanotube cytotoxicity using human keratinocyte cells**. *J Toxicol Environ Health A* 2003, **66**:1909-1926.

APPENDIX

Tables and Figures

A. Formalin/SPA Study

Table 1. Inspiratory dynamic lung compliance – effect of formalin exposure and SPa pretreatment

Group	(mL/cm H_2O)
Control	0.2942 (±0.0391)
Formalin	8.7353 (±5.1736)
Formalin + SPa	0.2614 (±0.0430)

Table 2. Lung permeability– effect of formalin exposure and SPa pretreatment

Group	(% lung clearance/min)
Control	0.4510 (±0.2754)
Formalin	2.3667 (±1.8144)
Formalin + SPa	0.3746 (±0.0621)

Table 3. Spots Rendered Undetectable by Formalin and Reappearing with SPa Pretreatment

Spot#	Swiss-Prot	Name /Description
8516	Q3U3S3	Cenpl, centromere protein L
1604	Q5DQJ3	Capza2, F-actin capping protein alpha-2 subunit
8523	O88569	Sept-9, Septin-9
8507	Q6URK4	hnRNPA3, heterogeneous nuclear ribonucleoprotein A3 variant b
1302	P19527	Nefl, neurofilament protein
2320	P16086	Sptan1, spectrin, alpha, non-erythrocytic 1
8303	Q5PQN7	Lzic, leucine zipper & ICAT homologous domain-containing
8203	Q02975	Znf354a, Zinc Finger 354a

Table 4. Proteins Decreased by Formalin, an Effect Prevented by SPa pretreatment

1300003B13Rik protein	Leucine zipper/CTNNBIP1
Annexin 1	Mannose-binding protein A precursor
Centromere protein L	Neurofilament triplet L protein
Dimethylarginine dimethylaminohydrolase 1	Peroxiredoxin 1
E3 ubiquitin protein ligase	Rfng protein
Hemoglobin alpha chain	Similar to SPAC12B10.16c
Heterogeneous nuclear ribonucleoprotein A2/B1	SH3-domain GRB2-like 3
Heterogeneous nuclear ribonucleoproteinA3 variant b	Sodium channel beta 3 subunit
Hyaluronidase	

Table 5. Proteins increased by formalin, an effect prevented by substance P pretreatment

ATP synthase beta subunit	Hemoglobin beta chain, major, Type I
Basigin	Keratin KA19
Biliverdin reductase A	Kv4 K channel-interacting protein
Calgranulin A	Mta3 protein
Catalase	Myosin light polypeptide 6
Cellular Retinol Binding Protein (Crbp)	Protective protein for beta-galactosidase
Cytokeratin-8	Pyruvate dehydrogenase kinase
E-septin	Ras-related protein Rab-25
Fatty acid binding protein 5	Salt-tolerant protein
Hemoglobin, alpha 1	Tropomyosin alpha chain

Table 6. Other protein effects

unaffected by formalin increased by pretreatment with Spa	Schlafen2
unaffected by formalin, decreased by pretreatment with SPa	E-septin short form L-gulono-gamma-lactone oxidase
present in Control and Formalin groups, missing in the substance P group	Polyubiquitin
visibly charge-modified/increased in formalin, prevented by substance P pretreatment	Selenium binding protein 2 Biliverdin reductase A
other	Fibrinogen alpha and beta

Table 7. Changes in protein levels greater than 10-fold as a result of formalin exposure and SPa pre-treatment + Formalin compared to control levels

Name	Description	Formalin	SPa + Formalin	Location/Type
CAPZA2	capping protein (actin filament) Z-line	↓-37.79	↑1.76	cytoplasm
CENPL	centromere protein L	↓-117.76	↑1.48	nucleus
CNOT8	CCR4-NOT transcription complex, subunit 8	↑31.40	No Change	nucleus/transcription
DPYSL2	dihydropyriminase-like 2	↑1.58	↓-64.19	cytoplasm/enzyme
FGA	fibrinogen alpha chain	No Change	↑185.53	extracellular space
HBA2	hemoglobin, alpha 2	↑12.44	↑6.34	cytoplasm/transporter
HMGB4	high mobility group box 4	No change	↑151.79	nucleus/transcription
HNRNP	heterogeneous nuclear ribonucleoprotein A2/B1	↓-79.25	↑3.05	nucleus
	heterogeneous nuclear ribonucleoprotein A3	↓-29.46	↑2.44	nucleus
	heterogeneous nuclear ribonucleoprotein C (C1/C2)	↑110.83	No Change	nucleus
KCNIP1	Kv channel interacting protein 1	↑4.88	↓-10.83	plasma membrane/ion channel
KRT8	keratin 8	↑1.12	↓-37.71	cytoplasm/kinase
LZIC	leucine zipper, CTNNBIP1 domain containing	↓-59.90	↑6.53	nucleus/plasma membrane
NEF1	neurofilament light polypeptide 68kDa	↓-57.03	↑2.46	cytoplasm
PDK1	pyruvate dehydrogenase kinase, isozyme 1	↑1.05	↓-10.40	cytoplasm/kinase
PRMT2	protein arginine methyltransferase 2	↓-46.83	↑1.92	nucleus/enzyme
SEPT9	septin 9	↓-4.10	↓-10.93	cytoplasm/enzyme
SPTAN1	spectrin, alpha, non-erythrocytic 1	↓-11.66	↑9.60	plasma membrane
TUBB3	tubulin, beta	↑138.77	No Change	cytoplasm
UBB	ubiquitin B	↑4.52	↓-519.3	cytoplasm
VIM	vimentin	No Change	↑184.98	cytoplasm
ZNF354a	zinc finger protein 354A	No Change	↑371.03	nucleus/transcription

Table 8. Ontological Analysis Identifying Biological Functions Associated with Formalin Exposure and Possibly Attenuated by Pre-treatment with SPA

Function/Disease	Formalin	SPA + Formalin	Score	# of Molecules
Cell signaling pathway	↑ACTB, ↓ANXA1, ↓APOA1, ↑ATP5B, ↓BLVRA, ↑CAT, ↓CAV1, ↑CCNE, ↑CHEK1, ↑DPYSL2, ↑FABP5, ↑FGA, ↓HSPA8, ↑KCNIP, ↑LCK, ↓NEFL, ↑PDK1, ↓PRMT2, ↑RBP1, ↓RFN, ↓SPTAN, ↑TPM1, ↑TRIP10, ↑UBB	↑ACTB, ↑ANXA1, ↓APOA1, ↓ATP5B, ↓BLVRA, ↓CAT, ↑CAV1, ↑CCNE, ↑CHEK1, ↓DPYSL2, ↓FABP5, ↑FGA, ↓HSPA8, ↓KCNIP, ↓LCK, ↑NEFL, ↓PDK1, ↑PRMT2, ↓RBP1, ↓RFN, ↑SPTAN, ↓TPM1, ↓TRIP10, ↓UBB	16	24
Cell death	↓ANXA1, ↓APOA1, ↓BLVRA, ↑BS, ↑CAT, ↓CAV1, ↑CCNE, ↑CHEK1, ↑HBA2, ↑HNRP, ↓HSPA8, ↑KRT, ↑LCK, ↓NEFL, ↑PDK1, ↓POL, ↓PRMT2, ↑S100A8, ↑TPM1, ↑TRIP10	↑ANXA1, ↓APOA1, ↓BLVRA, ↓BS, ↓CAT, ↑CAV1, ↑CCNE, ↑CHEK1, ↑HBA2, ↑HNRP, ↓HSPA8, ↓KRT, ↓LCK, ↑NEFL, ↓PDK1, ↓POL, ↑PRMT2, ↑S100A8, ↓TPM1, ↓TRIP10	15	20
Apoptosis	↓ANXA1, ↓BLVRA, ↑CAT, ↓CAV1, ↑CCNE, ↑CHEK1, ↑HBA2, ↑HNRP, ↓HSPA8, ↑KRT, ↑LCK, ↓NEFL, ↑PDK1, ↓POL, ↓PRMT2, ↑S100A8, ↑TPM1	↑ANXA1, ↓BLVRA, ↓CAT, ↑CAV1, ↑CCNE, ↑CHEK1, ↑HBA2, ↑HNRP, ↓HSPA8, ↓KRT, ↓LCK, ↑NEFL, ↓PDK1, ↓POL, ↑PRMT2, ↑S100A8, ↓TPM1	12	17
Tumorigenesis/ neoplasia	↑ACTB, ↓ANXA1, ↓CAV1, ↑CCNE, ↑CHEK1, ↑DPYSL2, ↑FABP5, ↑HBA2, ↓HSPA8, ↑KRT1, ↑LCK, ↓POL, ↑S100A8, ↓SEPT9, ↑TPM1, ↑TUBB, ↑VIM	↑ACTB, ↑ANXA1, ↑CAV1, ↑CCNE, ↑CHEK1, ↓DPYSL2, ↓FABP5, ↑HBA2, ↓HSPA8, ↓KRT1, ↓LCK, ↓POL, ↑S100A8, ↓SEPT9, ↓TPM1, ↑TUBB, ↑VIM	13/11	17/15
Inflammatory disorder	↓APOA1, ↑BS, ↓CAV1, ↓HNRPA3, ↓HSPA8, ↓HYAL, ↑KRT, ↓POL, ↑S100A8, ↓SFTPA1, ↓SLFN, ↑TUBB, ↑VI	↓APOA1, ↓BS, ↑CAV1, ↑HNRPA3, ↓HSPA8, ↑HYAL, ↓KRT, ↓POL, ↑S100A8, ↑SFTPA1, ↑SLFN, ↑TUBB, ↑VI	11	13
Proliferation	↓ANXA1, ↑BS, ↑CAT, ↓CAV1, ↑CCNE, ↑CHEK1, ↑CNOT, ↑FABP5, ↓GUL, ↓HNRPA2B, ↑KRT, ↑LCK, ↑S100A8, ↓SLFN, ↑VI	↑ANXA1, ↓BS, ↓CAT, ↑CAV1, ↑CCNE, ↑CHEK1, ↑CNOT, ↓FABP5, ↓GUL, ↑HNRPA2B, ↓KRT, ↓LCK, ↑S100A8, ↑SLFN, ↑VI	10	15
Growth	↑ACTB, ↓ANXA1, ↑ATP5B, ↑BS, ↑CAT, ↓CAV1, ↑CCNE, ↑HNRP, ↑TPM1	↑ACTB, ↑ANXA1, ↓ATP5B, ↓BS, ↓CAT, ↑CAV1, ↑CCNE, ↑HNRP, ↓TPM1	5	9

Table 9. Differentially Expressed Proteins in Canonical Pathways

Pathway	Name	Description	Formalin Fold-Change	SPA + Formalin Fold-Change
Acute Phase Response Signaling (p=0.0000175)				
	APOA1	Apolipoprotein A-I	-3.11	-1.22
	FGA	Fibrinogen alpha chain	None	+185.53
	PDK1	Pyruvate dehydrogenase kinase. isozyme 1	+1.06	-10.40
	RBP1	Retinol binding protein 1. cellular	+1.70	-2.36
NRF-2 mediated oxidative stress response (p=0.000582)				
	ACTB	Actin. beta	+1.26	+2.35
	CAT	Catalase	+1.74	-2.58
	UBB	Ubiquitin B	+4.52	-519.30
Cell Cycle: G2/M DNA damage checkpoint regulation (0.000635)				
	CHEK1	CHK1 checkpoint homolog (*S. pombe*)	+4.507	+8.03
	UBB	Ubiquitin B	+4.520	-519.30

Table 10. Top Scoring Networks for Formalin and SPa Treatment Groups

Function/ Disease	Formalin	SPA + Formalin	Score	Number of Molecules
Development/ Tissue Cancer	Network 1 14-3-3 [illegible] ACTB Actin Akt ANXA1 Ap1 APOA1 ATP5B BLVRA BSG [illegible] CAT CAV1 CHEK1 DPYSL2 F Actin FABP5 HNRNPC Insulin Jnk KRT8 KRT19 LCK Mapk NEFL [illegible] NFkB PDK1 PI3K Pkc(s) RBP1 S100A8 TPM1 TUBB3 VIM	Network 1 14-3-3 [illegible] ACTB Actin Akt ANXA1 Ap1 APOA1 ATP5B BLVRA BSG [illegible] CAT CAV1 CHEK1 DPYSL2 F Actin FABP5 HNRNPC Insulin Jnk KRT8 KRT19 LCK Mapk NEFL [illegible] NFkB PDK1 PI3K Pkc(s) RBP1 S100A8 TPM1 TUBB3 VIM	Formalin-51 SPa-51	Formalin-22 SPa-22
Cell death	Network 2: Cell death, Reproductive System BIRC4 BTG2 CAPZA2 Caspase CAT CCNE1 [illegible] CSF1 CSF2 DDAH1 FGF2 FOS GFAP HBA1 HBA2 HBB (includes EG:3043) HBB-AR HBE1 HBG1 HBG2 HBQ1 (includes EG:[illegible]) HBZ heparin HNRNPC HNRNPU HYAL3 hyaluronic acid IL1B KRAS NOTCH1 P38 MAPK PDGF BB RFNG SELENBP1 SLFN2 Network 3: Cell death, Neurological disease BDNF BTG1 BTG2 Ca2+ CASP3 CAT CDKN2A CEBPA [illegible] CLTA [illegible] D-glucose DNAJC13 FANCA GAK [illegible] heparin HGF HMGB1 (includes EG:29459) HNRNPA2B1 HNRNPC Hsp90 HSPA8 HSPH1 [illegible] MYB [illegible] PEX19 POLB SFTPA1 (includes EG:20387) SPTAN1 [illegible] TRIP10 UBB UBE2 [illegible] Network 4: Cell death, Cell Cycle, Gene Expression amino acids APP CDKN1A CLU CTSA F2 F3 FGA FN1 GLB1 HNRPA3 ID2 ITGAM MMP12 MMP13 NFKB1 NFKBIA PAK2 PAX3 PGR PPARG PRMT2 RARA RB1 RELA retinoic acid RXRA S-adenosylmethionine SEPT9 SOX4 TGFB1 TNC TRPC1 TYRP1 YWHAE	Network 2: Cell death, Reproductive System BIRC4 Ca2+ CASP1 CASP4 CDKN2A CEBPA CLTA D-glucose DDB2 HGF Histone h3 HNRNPA2B1 Hsp90 HSPA8 IL3 KPNB1 LMNA MYB NFE2L2 PEX19 PKN1 POLB SFTPA1 (includes EG:20387) SPTAN1 TGFA THBS1 TP53 TRIM28 TRIP10 TWIST1 UBB UBE1L2 Ubiquitin VIM XPC	Formalin – 21, 21, 8, 2 SPa – 16, 2	Formalin – 11, 11 (5 with FGA) SPa – 10, 3
Inflammatory Disease	None	Network 2 CAPZA2 CASP4 Caspase CGLP [illegible] CCNE1 DDAH1 FGF2 FOS HBA2 HBB (includes EG:3042) Histone h3 HYAL3 hyaluronic acid IL3 IL1B KRAS LMNA MMP3 MMP12 MMP13 MMP14 NFE2L2 NOTCH1 P38 MAPK PDGF BB PDGF AA PLA2G4A PLAU RFNG SELENBP1 SLFN2 SPARC THBS1 TWIST1 VIM	SPa – 18	SPa – 15
Cell to cell signaling	None	Network 4 APP CTSA F2 F3 FGA FN1 GLB1 Histone h3 HNRPA3 ID2 IL6 ITGAM Jnk MMP12 MMP13 MMP14 PAK2 PAX3 PLAU PLG PPARA PTK [illegible] PRMT2 RB1 retinoic acid RHOA SEPT9 SOX4 S-adenosylmethionine TGFB1 THBS1 TNC TRPC1 TYRP1 YWHAE	SPa – 8	SPa – 5
Post-translational modification	Network 6 BTG1 BTG2 CNOT10 CNOT8 CNOT10		Formalin 2	Formalin 1

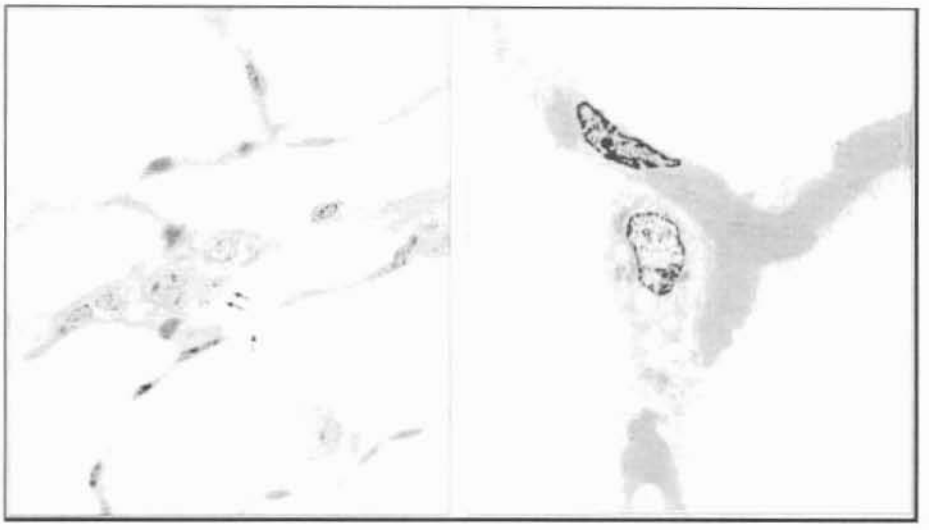

Figure 1. This photomicrograph of excised lung tissue reveals injury to the alveolar-capillary membranes (arrows) and cell destruction in the formalin rats (left) compared to the SPa-treated rat (right).

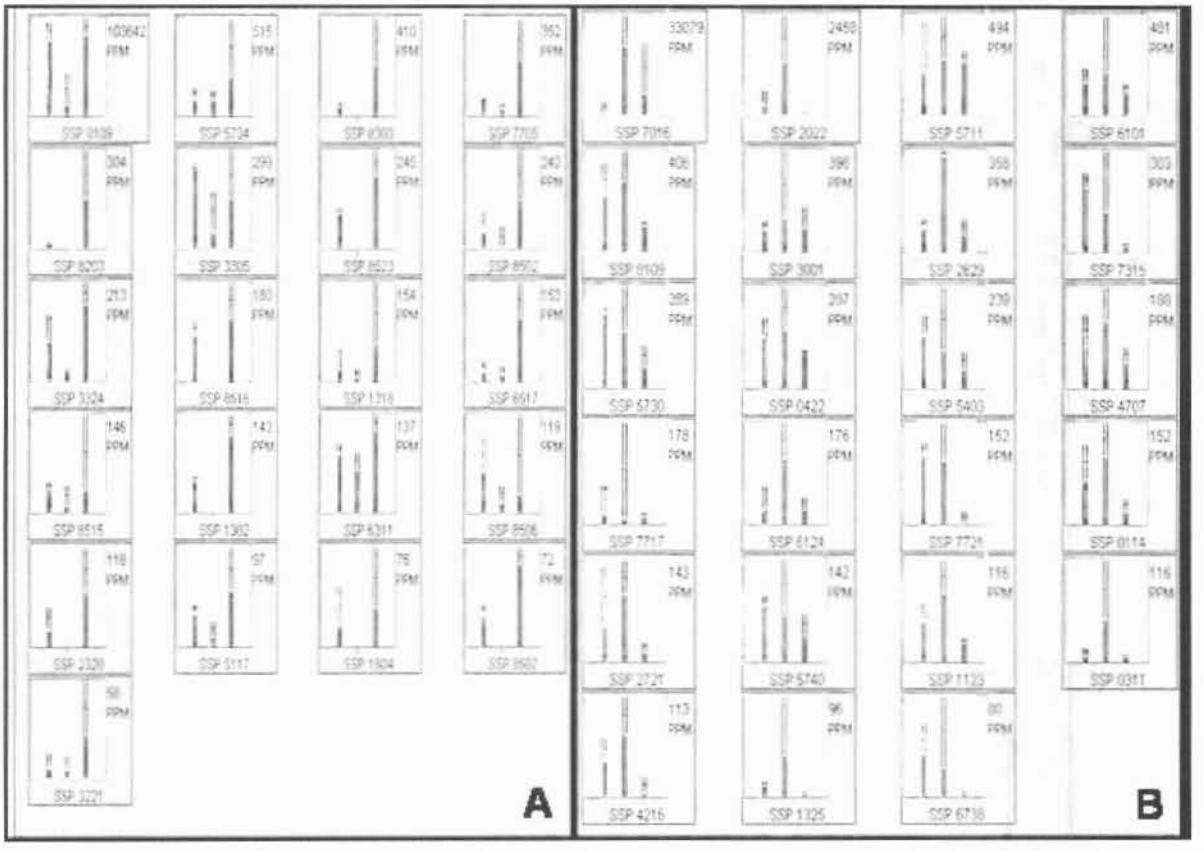

Figure 2. Panel 2a illustrates a graphic representation of expression changes in the 21 proteins. The leftmost bar is Control, center is Formalin, and rightmost is SPa /Formalin. Panel 2b shows a subset of proteins up-regulated by formalin treatment, a change prevented by SPa pretreatment. Twenty-three of the 71 spots were classified under this category.

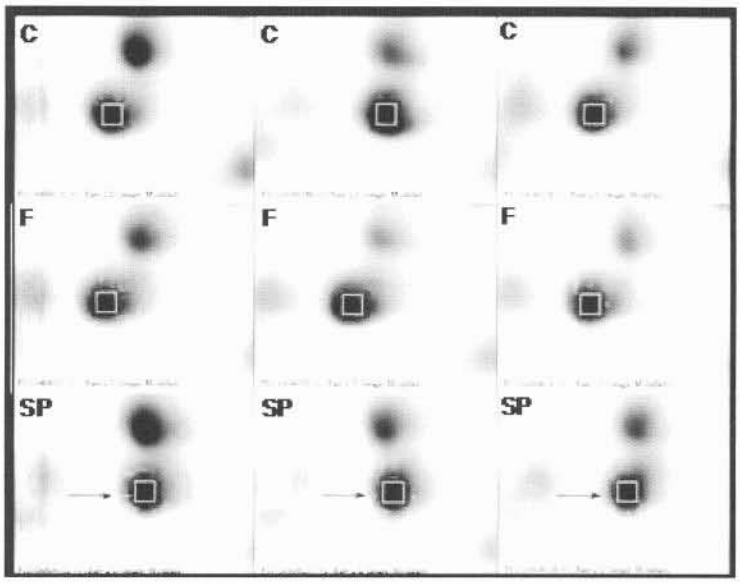

Figure 3. Scanned images of 2-DE gels from the three experimental groups. An example of protein expression changes is spot 5711, identified as selenium binding protein 2. It has shifted, but the spot position is slightly ambiguous in the control group. In the formalin treated, the spot is more acidic (toward the left edge of the gel), while in the SPa treated group the spot is more basic (right edge of gel).

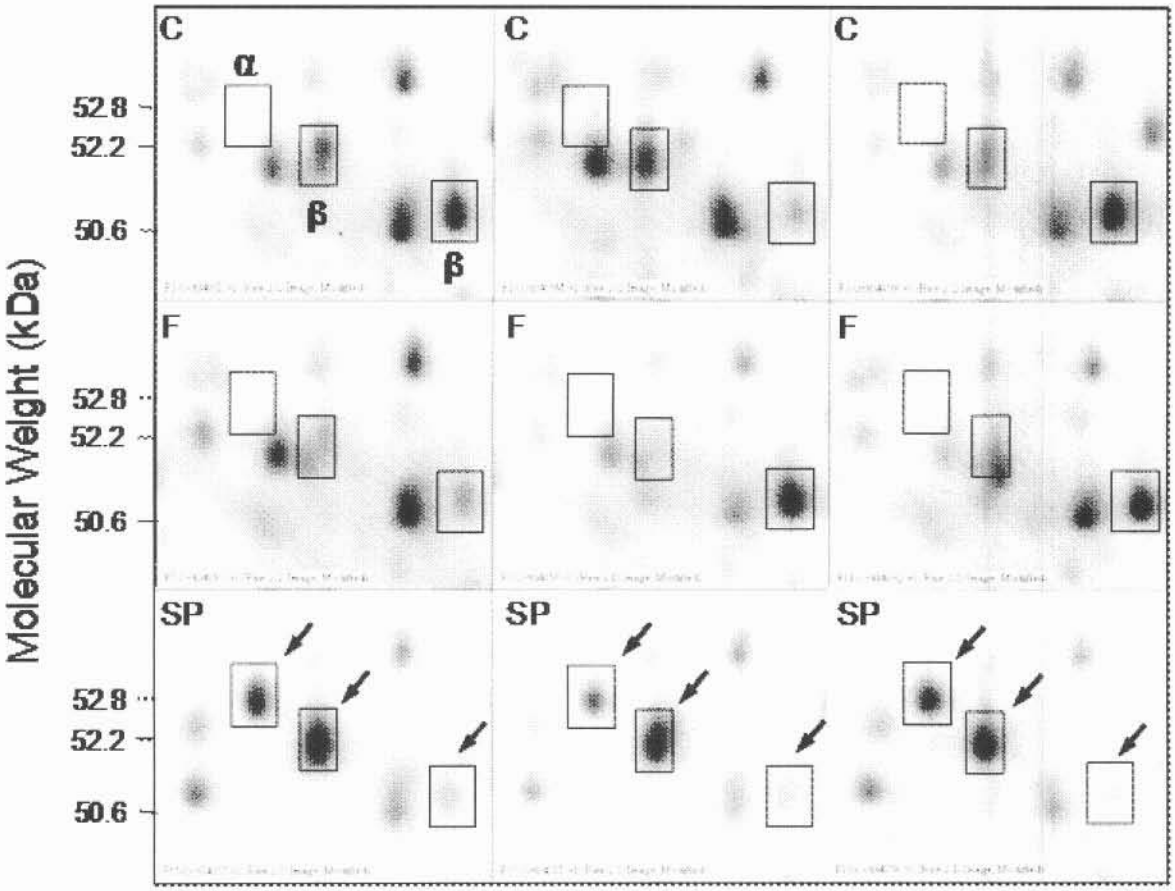

Figure 4. Fibrinogen subunits identified on the 2-DE gel. Alpha and Beta subunits are labeled with boxes in the control, formalin only, and SPa treated groups. Formalin had little, consistent effect on lung fibrinogen, while the substance P pretreatment changed the type of fibrinogen found in the lung tissue. Alpha fibrinogen was induced by SPa pretreatment. Beta fibrinogen seems to have undergone a mass increase from 50.6 kDa to 52.2 kDa and an apparent increase in abundance with SPa.

B. JP-8 Type II Alveolar Cell Study

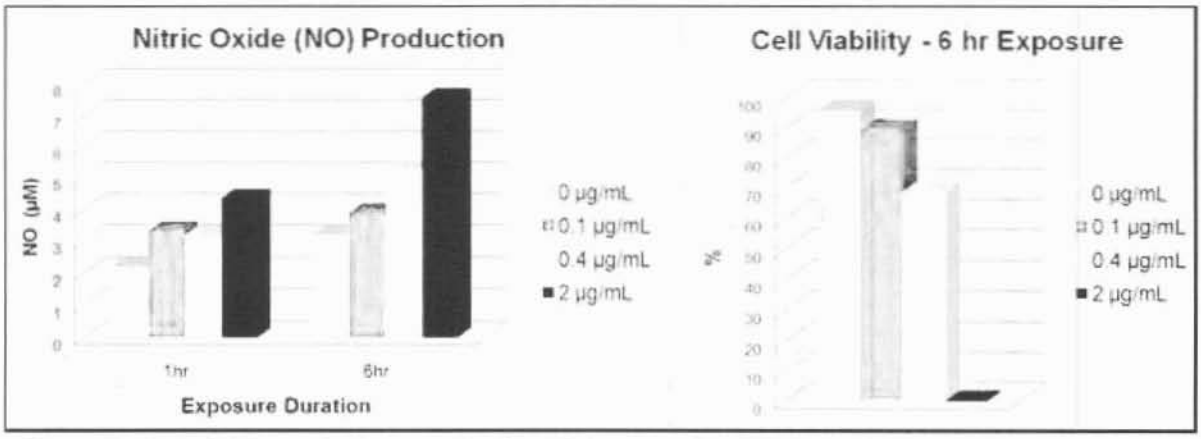

Figure 5. Nitric Oxide production was significantly increased by JP-8 in both 1 h and 6 h exposures; Cell viability was unaffected by 1 h JP-8 exposure; 0 viability at 6 h, 2.0 µg/mL

Table 11. Protein Expression Differences, 1 hour vs. 6 hour Controls

Rank	IPI	Protein	Fold Change 1-6 h	q
24	IPI00188909.2	collagen alpha-1(I) chain precursor	1.28	0.0003
95	IPI00476804.2	collagen, alpha-1 type I	1.24	0.0003
53	IPI00844828.1	procollagen, type I, alpha 1	1.29	0.0005
362	IPI00454263.1	annexin A3 (LRRGT00047)	1.35	0.0006
399	IPI00207390.7	annexin A3	1.29	0.0006
198	IPI00763106.1	similar to Fascin	1.18	0.02
416	IPI00193279.1	ornithine aminotransferase	1.19	0.04

Table 12. Priority 1 Proteins Up-regulated by JP-8 exposure (≥1.5-fold; Q≤0.05)

	0.1 µg/mL	0.4 µg/mL	2.0 µg/mL
1 hour	0 (0)	0 (0)	0 (0)
6 hour	0 (0)	0 (55)	0 (69)

Values in parentheses include both priority 1 and priority 2 IDs

Table 13. Priority 1 Proteins Down-regulated by JP-8 exposure (≥1.5-fold; Q≤0.05)

	0.1 µg/mL	0.4 µg/mL	2.0 µg/mL
1 hour	0 (0)	1 (2)	2 (3)
6 hour	20 (36)	137 (185)	384 (649)

Values in parentheses include both priority 1 and priority 2 IDs

Table 14. Protein Groups Down-regulated by @ 6 hr by 2.0 µg/mL JP8			
Protein	**Members**	**Ave. Fold Change**	**Ave. # of Peptide Seq.**
14-3-3 gamma (zeta/delta, epsilon, eta, theta)	4	-2.00	6
26S protease regulatory subunit (6B, 7, 13)	3	-1.85	2
40S ribosomal protein	19	-1.87	3
60S acidic ribosomal protein (P1, P2a, P2b)	3	-1.60	5
60S ribosomal protein	10	-1.92	3
actin or actin-related	24	-1.86	15
AHNAK nucleoprotein (desmoyokin)	8	-1.90	28
aldose reductase	4	-1.68	7
collagen/collagen-related	14	-1.84	8
dynein and spectrin	5	-1.77	2
eukaryotic translation elongation factors	13	-2.28	8
glyceraldehyde-3-phosphate dehydrogenase	14	-2.02	4
GTP-binding proteins (Ras, Rab, Ran, etc.)	17	-1.82	3
heat shock proteins	21	-1.84	8
pyruvate kinase	7	-1.98	14
ribosomal protein (other)	11	-1.87	2
splicing factors	10	-1.71	2
tubulin	18	-2.09	11
ubiquitin-related	10	-1.74	2

Groups include proteins with 3 or more isoforms detected or related proteins; Average Fold Change for 6 h Control vs. 6 h 2.0 µg/mL exposure

Table 15. Proteins down-regulated (q≤0.05) at 6 h by 0.1 µg/mL JP-8; GO distribution of altered proteins.

IPI	ENTREZ GENE ID	RGD	Annotation
IPI00191142.1	81773	RGD:621024	40S ribosomal protein S10
IPI00191142.1	81773	RGD:621024	40S ribosomal protein S10; 17 kDa protein
IPI00373448.3	81773	RGD:621024	40S ribosomal protein S10; 18 kDa protein
IPI00366014.3	684988	RGD:621027	40S ribosomal protein S13
IPI00392390.2	83789	RGD:619887	40S ribosomal protein S2
IPI00214582.1	29258	RGD:61907	40S ribosomal protein S7
IPI00358285.2	290678	RGD:1559708	ribosomal protein S10
IPI00203523.1	360572	RGD:1304897	60S ribosomal protein L23a
IPI00204703.5	29345	RGD:69302	47 kDa heat shock protein (serpin H1 precursor; collagen-binding protein)
IPI00324539.6	286758	RGD:628763	aquaporin-11
IPI00569197.2	501389	RGD:1588387	chromosome 9 open reading frame 36 (LOC501389)
IPI00388632.3	307492	RGD:1310695	dead end homolog 1 (52 kDa protein)
IPI00371802.3	304719	RGD:1560340	excision repair cross-complementing rodent repair deficiency, complementation group 4
IPI00200757.1	25661	RGD:2624	fibronectin precursor, Isoform 1
IPI00368017.4	691044	RGD:1359558	GTPase activating protein testicular GAP1
IPI00210090.3	117280	RGD:620372	heterogeneous nuclear ribonucleoprotein U (SP120)
IPI00211813.1	79433	RGD:71000	myosin heavy chain (Neuronal)
IPI00360637.3	310178	RGD:1307193	myosin-10 (Myosin heavy chain, nonmuscle IIb) (Cellular myosin heavy chain, type B)
IPI00558912.1	24582	RGD:3136	myosin-11
IPI00367479.4	308572	RGD:1306821	myosin-14
IPI00209113.3	25745	RGD:3140	myosin-9
IPI00370406.2	679306	RGD:1623873	NMDA receptor-regulated gene 2, isoform 2
IPI00394392.3	56768	RGD:69406	piccolo (presynaptic cytomatrix protein)
IPI00464535.1	246303	RGD:619907	plasminogen activator inhibitor 1 RNA-binding protein, isoform 2)
IPI00359590.5	308918	RGD:1565383	protein tyrosine phosphatase, receptor-type, F interacting protein, binding protein 2
IPI00202873.1	24718	RGD:3553	reelin precursor, isoform 1
IPI00203078.1	116475	RGD:620744	selective LIM binding factor, rat homolog
IPI00191416.1	79111	RGD:708535	solute carrier family 27 (fatty acid transporter), member 5 (bile acyl-CoA synthetase)
IPI00779007.1	310360	RGD:1566344	translation elongation factor 1 alpha 1 (50 kDa protein)
IPI00195372.1	171361	RGD:67387	translation elongation factor 1-alpha 1
IPI00568311.1	171361	RGD:67387	translation elongation factor 1-alpha 1C; 46 kDa protein
IPI00195372.1	171361	RGD:67387	translation elongation factor EF-1, subunit alpha 1 (50 kDa protein)
IPI00325281.1	24799	RGD:3781	translation elongation factor EF-1, subunit alpha 2 (45 kDa protein)
IPI00568311.1	171361	RGD:67387	translation elongation factor Tu
IPI00372810.4	292148	RGD:1307269	translation initiation factor 3, subunit 10 (theta) (ZH12 protein)
IPI00373703.2	301079	RGD:1311745	uncharacterized protein KIAA1143 homolog

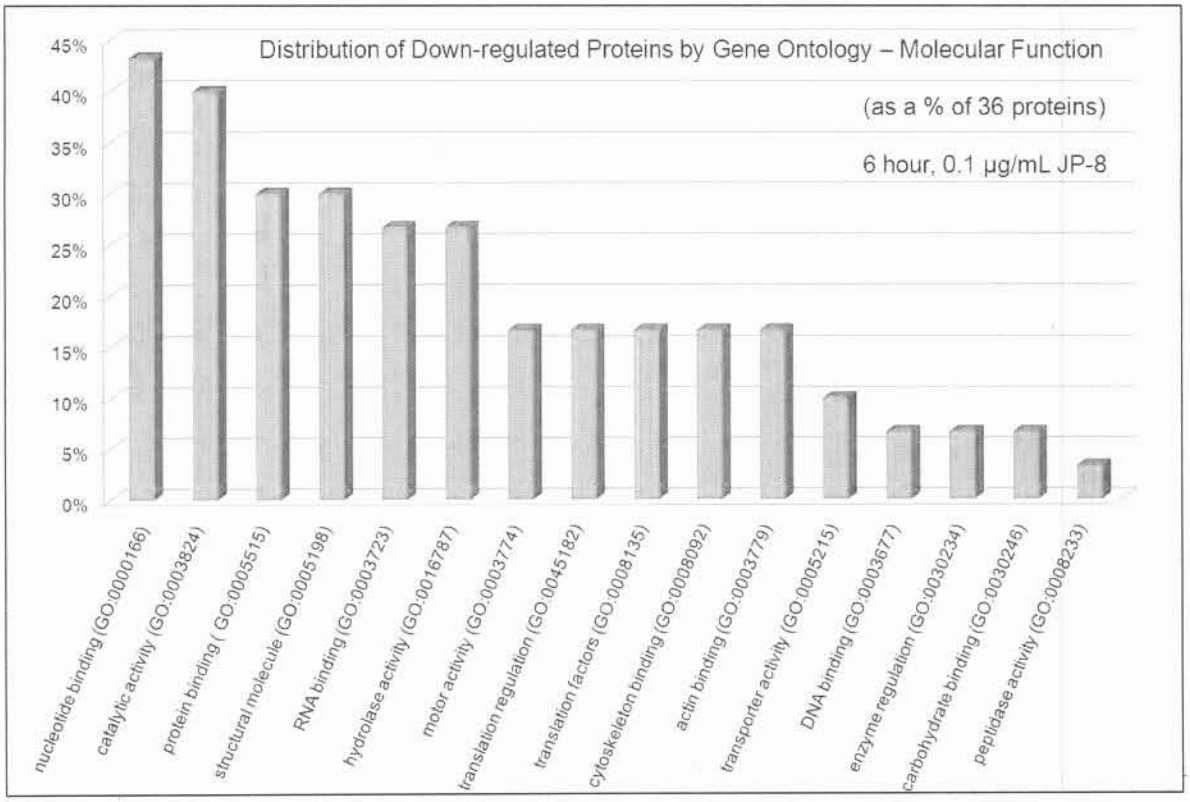

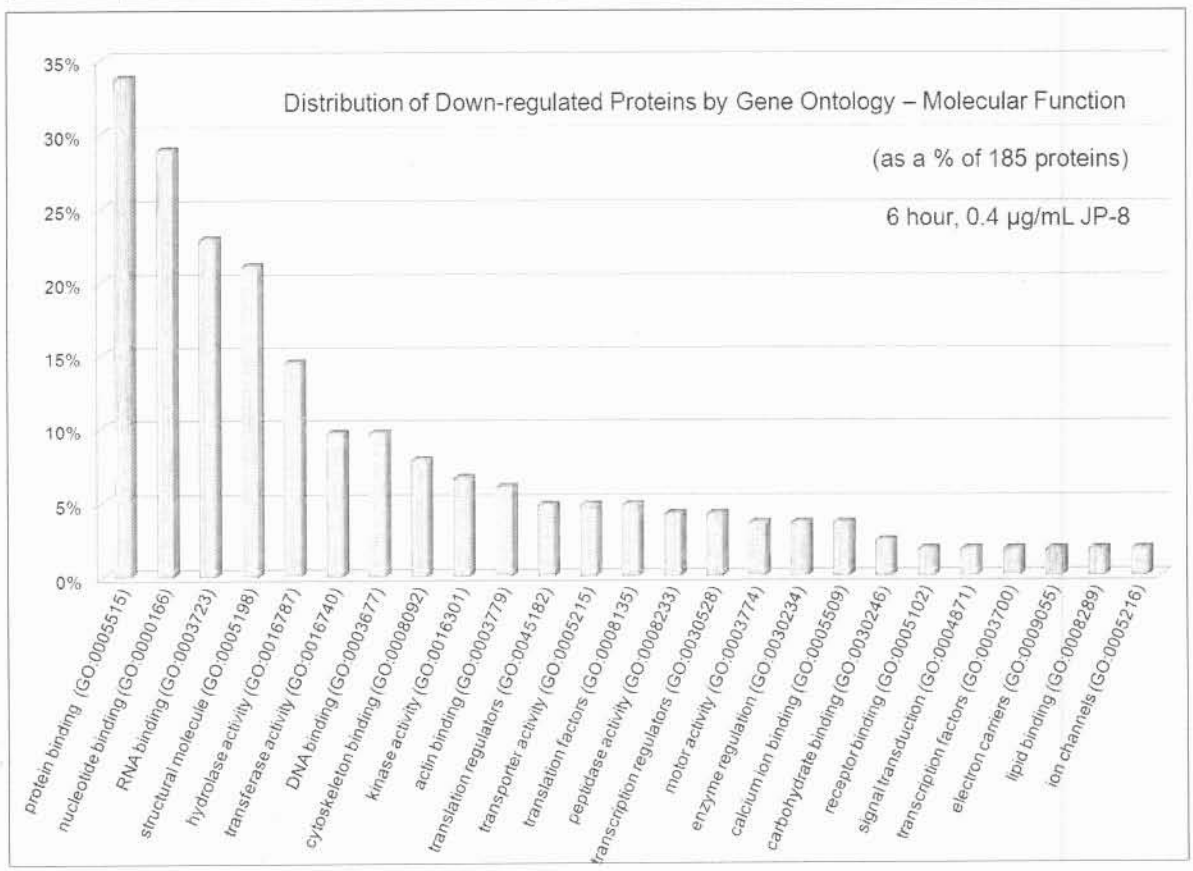

Figures 6 and 7.

C. Carbon Nanoparticle Study

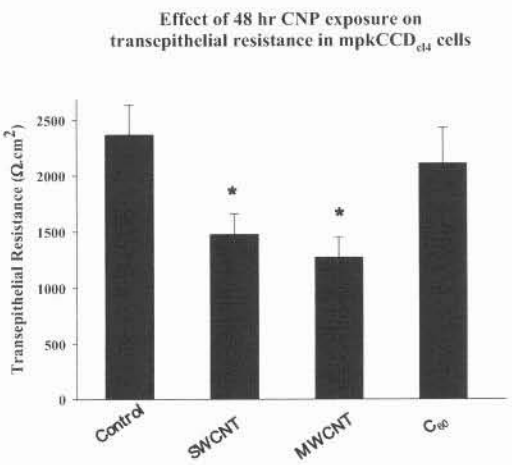

Figure 8. Effect of 48 hour CNP exposure on transepithelial resistance in mpkCCD$_{cl4}$ cells. Confluent monolayers of mpkCCD$_{cl4}$ cells were incubated for 48 hours with 20 μg/cm^2 CNP as indicated. Cells were removed from the Transwell chambers and mounted in Ussing chambers to monitor transepithelial electrical resistance. Bars indicate S.E.M. *Significantly different from matched control cultures (P< 0.02).

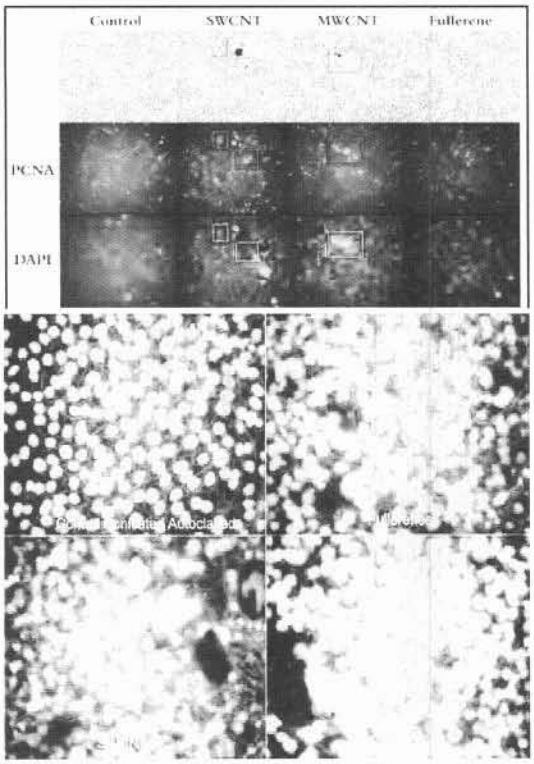

Figure 9. Top panel: mpkCCD$_{cl4}$ cells were grown to confluence in 6-well plates and then treated with sonication-suspended CNP at 20 μg/cm^2 for 48 hours. The cells were fixed and stained with proliferating cell nuclear antigen (PCNA) to indicate the nuclei of proliferating cells and with DAPI to stain all cell nuclei. The red boxes depict areas of CNP agglomeration and are the same in all fields. Bottom panel: mpkCCD$_{cl4}$ cells were seeded in 6-well plates and exposed for seven days to low levels (4 μg/cm^2) of the indicated nanopartical. The medium (containing fresh CNP) was renewed 3 times. The cells were fixed and actin was visualized using rhodamine-phalloidin (red) while the nuclei were stained with DAPI (blue). Cells treated with CNP showed an increased number of large, multinucleated cells.

Table 16. Proteins altered by ethanol-sterilized, non-sonicated SWNT and MWNT at 200 μg/cm^2 for 24 h, separated and analyzed by 2-DE and identified via mass spectrometry.

Increased expression of the proteins below, a response that may be directly or indirectly associated with cell proliferation and function	
Name	**Function**
stathmin-like 2	regulator of microtubule dynamics; renal expression is ↓ in with uranium toxicity
pseudouridine synthase 1	involved in protein synthesis, serves to stabilize required RNA conformations during translation
flotillin-2, isoform 1	scaffolding protein within caveolar membranes, functionally participating in formation of caveolae or caveolae-like vesicles; tethers growth factor receptors linked to signal transduction pathways, may also be involved in cell adhesion
Ran-binding protein 1	bi-directional transport of proteins and ribonucleoproteins through the nuclear pore complex, spindle formation, reassembly of the nuclear envelope; expressed at sites of mesenchymal/epithelial induction
enolase, 1 alpha	energy metabolism for proliferation; non-neuronal enolase is a diagnostic marker for many tumors

Decreased expression of the proteins below, a response that may be directly or indirectly associated with cell proliferation	
Name	**Function**
gap junction alpha-8	may contribute to minor changes observed in TEER
cyclin G2	acts as cell cycle inhibitors in certain cell types and may contribute in inducing cell cycle arrest
myotubularin-related protein 9	protein-tyrosine phosphatase that acts on the 2nd messenger IP3, localized on endosomes, and regulates intracellular vesicle trafficking and autophagy; dysregulation can effect trafficking (see stathmin-like 2)
olfactory receptor 586	part of the cell surface receptor mediated signal transduction process involving G-protein coupled receptors, including cyclic AMP and IP3 mediated processes
zona pellucida glycoprotein 4	cell adhesion molecule; intracellular matrix; may be involved in ↓ TEER
protein kinase, cAMP dependent regulatory, type I, alpha	in PRKAR1A mutant cells (↓ functional kinase) there is an increase in DNA transcription and/or activation of other pathways leading to abnormal growth and proliferation

Table 17. Proteins altered by autoclave sterilized, sonication-suspended C_{60}, SWCNT, or MCWNT at 20 μg/cm^2 for 48 h versus Control, analyzed by label-free quantitative mass spectrometry.

Name	C_{60}	SWCNT	MWCNT
acyloxyacyl hydrolase	↓	-	↓
alpha-kinase 3	-	↓	↓
catenin, β like 1			
chaperonin containing Tcp1, subunit 3 (γ)	↑	-	-
creatine kinase, mitochondrial 1, ubiquitous	↓	-	-
cytoskeleton associated protein 5	-	↑	-
F-box and leucine-rich repeat protein 13	-	↑	-
ferritin light chain 1	-	↓	-
ferritin light chain 2	-	↓	-
GrpE-like 1, mitochondrial	↓	-	-
GTPase activating RANGAP domain-like 3	-	↑	-
hydroxyacyl-Coenzyme A dehydrogenase/3-ketoacyl-Coenzyme A thiolase/enoyl-Coenzyme A hydratase (trifunctional protein), β subunit	-	↑	↑
isocitrate dehydrogenase 3 (NAD+) β	-	↑	↑
olfactory receptor 584	↑	-	-
peptidylprolyl isomerase B	-	↓	-
phosphate cytidylyltransferase 1, choline, α isoform	↑	-	-
prostaglandin E synthase 3	-	↓	-
proteasome subunit, β type 7	-	↑	↑
protein phosphatase 2, catalytic subunit, α isoform	-	↑	-
protein phosphatase 2, catalytic subunit, β isoform	-	↑	-
protein tyrosine phosphatase, receptor type, B	↓	-	↓
protein tyrosine phosphatase, receptor type, R	-	-	↓
Ras-GTPase-activating protein SH3-domain binding protein 1	-	-	↑
ribosomal protein L30	-	↓	-
serine (or cysteine) peptidase inhibitor, clade B (Serpin B10)	-	↑	↑
similar to DEAD (Asp-Glu-Ala-Asp) box polypeptide 43	-	↓	-
sorting nexin 1	↑	-	-
SWI/SNF related, actin dependent regulator of chromatin c1	-	↑	↑
THO complex subunit 4, isoform 1	↑	-	-
transmembrane protein 202	↑	-	-
ubiquitin-conjugating enzyme E2 D2	↓	↓	↓
ubiquitin-like modifier activating enzyme 6	↓	↓	↓
voltage-dependent anion channel 2	↓	↓	↓
zinc finger, C3HC type 1	-	↑	-